Thin superconductors in a perpendicular magnetic ac field: General formulation and strip geometry

Ernst Helmut Brandt

Max-Planck-Institut für Metallforschung, Institut für Physik, D-70506 Stuttgart, Germany
(Received 16 November 1993)

The sheet current, electric field, and penetrating magnetic field in response to an applied perpendicular ac magnetic field are calculated for a thin type-II superconducting strip characterized completely by its sheet resistivity, which may be either nonlinear and frequency independent or linear, complex, and frequency dependent. The general formulation is given for the linear or nonlinear response of a strip and a circular disk in perpendicular time-varying magnetic field. An elegant and rapid numerical method is presented which solves this, in general, nonlinear one-dimensional integrodifferential equation with high precision on a personal computer and which accounts for the facts that the integral kernel has a logarithmic singularity and the sheet current for nearly ideal shielding (occurring at short times or high frequencies or for strong pinning of flux lines) has a one-over-square-root singularity near the specimen edges. As examples the linear Ohmic response of the strip to a sudden change of the applied field and to an ac field are given; Ohmic response is realized during flux flow or thermally activated flux flow. The complex magnetic susceptibility and the ac losses of the Ohmic strip are computed and approximated by simple expressions. This work completes the calculation of dissipation peaks in vibrating superconductors caused by various diffusion modes of the flux lines.

I. INTRODUCTION

The discovery of high-T_c superconductors (HTSC's) has revived the interest in experimental methods which measure the electromagnetic response of these extreme type-II superconductors in dc and ac magnetic fields $H_a(t)$. Most of these experiments are performed in *perpendicular geometry*, in which a thin ceramic or monocrystalline platelet or film is exposed to a magnetic field that has a component perpendicular to the specimen. This geometry gives a larger response since it generates a much a larger magnetic moment per unit volume than the longitudinal geometry. Two examples may illustrate this, in which we consider the maximum negative magnetic moment $-m$ achieved during complete flux expulsion, e.g., in the Meissner state of superconductors, or, with normal conductors, in high-frequency ac fields which penetrate only to a skin depth $\delta \ll d$:

(i) A circular disk of radius a and thickness $d \ll a$ in a perpendicular field H_a has $-m = (8a^3/3)H_a$ which is generated by a shielding sheet current $J(r) = (4/\pi)H_a r/(a^2 - r^2)^{1/2}$.[1,2]

(ii) A thin strip of width $2a$ and length $L \gg a$ has a moment $-m = \pi a^2 L H_a$ generated by a shielding sheet current $J(y) = 2H_a y/(a^2 - y^2)^{1/2}$ (see below).[3-5]

Both results are *independent of the thickness* d and mean large average magnetization or susceptibility $-m/(V H_a) = 8a/3\pi d$ (V = specimen volume) and $-m/(V H_a) = \pi a/2d$. In the longitudinal case where H_a is applied parallel to the specimen one always has the much smaller negative magnetization $-m/(V H_a) = 1$.

In perpendicular geometry, each volume element of the specimen is affected by not only the applied field but also a field caused by the magnetization of all other volume elements. These demagnetization effects can be described by a demagnetization factor N ($0 \leq N \leq 1$) if the specimen has the shape of an ellipsoid and if the magnetic response of the material is linear.[1] Both requirements are in practice never satisfied in experiments on HTSC's. In spite of this, demagnetization corrections are usually applied by approximating disks or strips with rectangular cross section by ellipsoids with half axes a and b, yielding demagnetizing factors $N = 1 - \pi b/2a$ for thin disks and $N = 1 - b/a$ for thin strips in perpendicular fields ($b \ll a$). The field at the equator of the disk or edge of the strip is then enhanced by a large factor $1/(1 - N)$; the same enhancement factor applies to the homogeneous effective magnetic field experienced by each volume element and to the magnetic moment as compared to the longitudinal geometry, which exhibits no demagnetization effects. Choosing the short axis b of the ellipsoid such that the correct magnetic moment is obtained, one gets $b = 3d/4$ for the disk and $b = 2d/\pi$ for the strip. Exactly the same result follows if one requires the volume or cross section of the ellipsoid to coincide with the volume of the disk or cross section of the strip, respectively.

The approximation by an ellipsoid, however, misses several real effects. First, at the sharp edges of rectangular samples the external field is enhanced even more, by a factor diverging as the logarithm of the radius of curvature of the edge, as follows from the theory of potentials by conformal mapping.[1,6] Second, the sheet resistance ρ/d of an ellipsoid with varying thickness $d(r) = d(0)(1 - y^2/a^2)^{1/2}$ is not constant but diverges at the edges if the specific resistivity ρ is constant (uniform material). Third, the realistic rectangular cross section causes a geometric surface barrier for the penetration

(but not for the exit) of magnetic flux even in type-I superconductors.[6,7] This barrier is due to the enhanced shielding current flowing in the edge region because this is thicker compared to the barrier-free elliptic cross section. The observed asymmetry of the irreversible magnetization curve in perpendicular geometry has often been misinterpreted as evidence for a Bean-Livingston barrier[8] for the penetration of flux lines through a planar surface.

The, usually tacit, assumption of an elliptic cross section yields spurious results in many cases. One example is the nonlinear static magnetization and the field and current profiles in the Bean critical state of a disk[2] or strip.[3,4] Another example is the linear magnetic response of a disk or strip treated in the present paper and in Ref. 9. Numerical computations of the magnetization and of field and current profiles in circular disks[10−13] usually do consider the correct rectangular cross section [see also the review papers, Ref. 14]. The profiles of the magnetic field component perpendicular to the plane of the disk or strip can be observed by magneto-optics.[15−18]

The present paper gives the general theory of the penetration of a time-dependent homogeneous applied field $H_a(t)$ into a thin strip or circular disk perpendicular to this field. This theory is then applied to the linear response of a thin strip and the results are compared with the results in longitudinal geometry. The present paper is Part I of a projected series. The forthcoming Parts II and III present explicit results for the circular disk and for square and rectangular plates.

In this work the coordinate perpendicular to the specimen plane is denoted by x. The principal quantity to be calculated is the sheet current

$$\mathbf{J}(y, z) = \int_{-d/2}^{d/2} \mathbf{j}(x, y, z) \, dx \ . \qquad (1.1)$$

The strip and the disk fill the space $|x| \leq d/2 \ll a$ and $|y| \leq a$, $|z| \leq L/2 \gg a$ or $r = (y^2 + z^2)^{1/2} \leq a$, respectively, (see the insets in Figs. 1 and 8 below) yielding sheet currents $\mathbf{J}(y, z) = -J(y)\hat{\mathbf{z}}$ (strip) and $\mathbf{J}(y, z) = -J(r)\hat{\phi}$ (disk, $\phi = $ polar angle). From the sheet current one obtains the magnetic moment $\mathbf{m}$ of the specimen

$$\mathbf{m} = \frac{1}{2} \int \mathbf{j} \times \mathbf{r} \, d^3 x \ , \qquad (1.2)$$

which points along $\hat{\mathbf{x}}$ and may be written in the form

$$\mathbf{m} = -\hat{\mathbf{x}} M L, \quad M = \int_{-a}^{a} y \, J(y) \, dy \quad \text{(strip)} \ , \qquad (1.3)$$

$$\mathbf{m} = -\hat{\mathbf{x}} M, \quad M = \pi \int_{0}^{a} r^2 \, J(r) \, dr \quad \text{(disk)} \ . \qquad (1.4)$$

The factor $1/2$ of the definition (1.2) has been dropped in the expression (1.3) for the magnetic moment per unit length of the strip, since one has to consider the contribution of the U turn of the sheet current at the far-away ends of the strip; since $\text{div} \mathbf{j} = 0$ or $\text{div} \mathbf{J} = 0$ the integrals over $z J_y(y, z)$ and $y J_z(y, z)$ are exactly equal and

contribute $\frac{1}{2}\mathbf{m}$ each.

The magnetic field generated by the sheet current follows from Ampère's law. For a thin strip one gets to an accuracy of d/a

$$\mathbf{H}(x, y) = \frac{1}{2\pi} \int_{-a}^{a} \frac{(y - u, -x, 0) \, J(u)}{(y - u)^2 + x^2} du \ + \mathbf{H}_a \ . \qquad (1.5)$$

Equation (1.5) yields the tangential components $H_z = 0$ and $H_y(d/2, y) = -H_y(-d/2, y) = \frac{1}{2} J(y)$ since $x/(u^2 + x^2) = \pi \, \text{sgn}(x) \, \delta(u)$ for $|x| \to 0$: the sheet current determines the jump of the tangential field H_y. For the perpendicular component $H_x(0, y)$ in the plane of the strip (i.e., inside the strip and outside the strip near its surfaces, or at arbitrary distance $|y|$ provided $|x| \ll a$) one gets

$$H_x(0, y) = H(y) = \frac{1}{2\pi} \int_{-a}^{a} \frac{J(u)}{y - u} du + H_a$$

$$= \frac{1}{2\pi} \int_{0}^{a} \frac{2u J(u)}{y^2 - u^2} J(u) \, du + H_a \ , \qquad (1.6)$$

where in the second expression the symmetry of the induced current $J(-y) = -J(y)$ has been used. In (1.6) and all similar integrals below, the interpretation is in the sense of Cauchy's principal value. In a similar way, the azimuthal (circumferential) sheet current $J(r)$ circulating clockwise in a thin disk generates a radial field at the disk surfaces $H_r(d/2, r) = -H_r(-d/2, r) = J(r)$, and a perpendicular field in the disk plane $x = 0$ (see also Ref. 2),

$$H_x(0, r) = H(r) = \frac{1}{2\pi} \int_{0}^{a} P(r, u) \, J(u) \, du, \qquad (1.7)$$

with the kernel

$$P(r, u) = \frac{K(k)}{u + r} + \frac{E(k)}{u - r}, \quad k = \frac{(4ur)^{1/2}}{u + r} \ . \qquad (1.8)$$

Here $K(k)$ and $E(k)$ are complete elliptic integrals of the first and second kind. Note that the integral kernels $2u/(y^2 - u^2)$ of (1.6) and $P(u, r)$ (1.8) are not symmetric in their two arguments but can be written in the form $y^{-1} f_1(y/u)$ or $r^{-1} f_2(r/u)$.

The above equations (1.1) to (1.8) describe the magnetostatics and do not contain any material parameter yet. When the magnetic field changes with time, an electric field E is induced which drives the sheet current according to Ohm's law. If the skin depth δ exceeds d (see below) then E is constant over the thickness and one has

$$J(y, z) = E(y, z) d(y, z) / \rho(y, z) \ . \qquad (1.9)$$

Here ρ/d is the sheet resistivity and ρ the electric resistivity averaged over the sample thickness ($\sigma = 1/\rho$ is averaged). In general, d/ρ may depend on the position, e.g., in inhomogenous specimens or if the thickness varies spatially. Note that the shape of the sample cross section enters only *here* but not in the magnetostatics above, since we consider the limit $d(y, z) \ll a$. Another, more frequent situation with spatially varying $\rho(y, z)$ is

encountered in type-II superconductors where the resistivity is caused by moving Abrikosov flux lines and in general depends on the local induction **B** and current density **j**. For our thin specimens in perpendicular field this means ρ depends on $B_x = \mu_0 H_x(y, z)$ and on the sheet current $J(y, z)$. If ρ depends on J, one has nonlinear resistivity, which may be caused by pinning and depinning of the flux lines at material inhomogeneities.

A large variety of measured B-, J-, and T-dependent resistivities of HTSC have been published (see, e.g., Ref. 19). For theories of thermal depinning I refer to the reviews, Refs. 20 and 21. With appropriately chosen $\rho(B, J)$, the equation of motion given below for the current density $J(x, t)$ in a slab in longitudinal fields (Sec. II) and for the sheet current $J(y, t)$ and $J(r, t)$ in a strip or disk in perpendicular field (Sec. III) may be used to compute flux creep (nonlinear flux flow) in the critical states of a slab or of a disk or strip described in Refs. 2-4.

In the examples of the present paper I shall concentrate on the equally interesting *linear* response of thin superconductors to a time-dependent applied perpendicular field $H_a(t)$. If required for linearity (in the flux-flow region one has, e.g., $\rho \sim B$), we assume a constant background field to which a small field $H_a(t)$ is added. The linear resistivity ρ_{ac} of a HTSC in general depends on the frequency $\omega/2\pi$ of the ac field. $\rho_{\text{ac}}(\omega)$ was calculated[22-25] taking into account the Meissner currents, elastic pinning, usual flux flow, and thermally assisted flux flow (TAFF[26,27]). Somewhat simplified (i.e., disregarding the contribution of normal electrons near T_c treated in Ref. 22, and assuming $\tau_{\text{TAFF}} \gg \tau_{\text{FF}}$) one has (in SI units)

$$\rho_{\text{ac}}(\omega) = i\omega\mu_0\lambda^2 + \rho_{\text{FF}} \frac{\tau_{\text{TAFF}}^{-1} + i\omega}{\tau_{\text{FF}}^{-1} + i\omega} . \quad (1.10)$$

Here λ is the magnetic penetration depth for currents parallel to the specimen surface; $\rho_{\text{FF}} \approx B\rho_n/B_{c2}$ is the flux-flow resistivity (ρ_n = normal resistivity, B_{c2} = upper critical field); $\tau_{\text{FF}} = B^2/\rho_{\text{FF}}\alpha_L$ is the relaxation time of the displaced flux-line lattice when this experiences a viscous-drag force density $-v\rho_{FF}/B^2$ and an elastic-pinning restoring force density $-u\alpha_L$ (u = flux-line displacement, α_L = Labusch parameter[28]); $\tau_{\text{TAFF}} \gg \tau_{\text{FF}}$ is the creep time. If the creep is thermally activated with activation energy U, one has $\tau_{\text{TAFF}} = \tau_{\text{FF}} \exp(U/k_BT)$. If the creep at low T is caused by tunneling of flux lines out from the pins one has $\tau_{\text{TAFF}} = \tau_{\text{FF}} \exp(S_E/\hbar)$ where S_E is the Euclidean action of the tunneling process.[20,29-31]

In the derivation[24,25] of (1.10) an exponential relaxation (creep) of a suddenly (at time $t = 0$) uniformly displaced flux-line lattice was assumed, yielding a relaxing Labusch parameter

$$\alpha_L(t) = \alpha_L \exp(-t/\tau_{\text{TAFF}}) . \quad (1.11)$$

In frequency space this means

$$\alpha_L(\omega) = \alpha_L i\omega/(\tau_{\text{TAFF}}^{-1} + i\omega) . \quad (1.12)$$

The same result follows from a force-balance equation, as in viscoelasticity.[25] However, recent ac experiments in Bi-Sr-Ca-Cu-O ceramics[32] indicate an *algebraic* relaxation law,

$$\alpha_L(t) = \alpha_L(1 + t/\tau)^{-\beta}, \quad (1.13)$$

which for $\omega\tau \ll 1$ yields the dispersion law

$$\alpha_L(\omega) = \alpha_L(i\omega\tau)^\beta\Gamma(1 - \beta) , \quad (1.14)$$

where $\Gamma(1 - \beta)$ is Euler's Gamma function. The authors of Ref. 32 find a nearly temperature-independent $\tau \approx 4 \times 10^{-12}$ s (for $\mu_0 H_a = 1$ T) and an exponent $\beta(T) \approx 1/(1 + U/k_BT)$ (see also Refs. 33, 34), and $\beta \approx 1$ for $T > 70$ K. Thus, $\Gamma(1 - \beta) \approx 1/(1 - \beta)$. With (1.14) one gets a complex resistivity (I assume $\tau > \tau_{\text{FF}}$ to get $\text{Re}\{\rho_{\text{ac}}\} \to \rho_{\text{FF}}$ for $\omega \to \infty$),

$$\rho_{\text{ac}}(\omega) = i\omega\mu_0\lambda^2 + \rho_{\text{FF}} \frac{i\omega\tau_{\text{FF}}}{i\omega\tau_{\text{FF}} + (i\omega\tau)^\beta\Gamma(1 - \beta)} . \quad (1.15)$$

The frequency-dependent linear resistivity $\rho(\omega, B, T)$ (1.10) and (1.15) may be used in the equations of motion for current and field derived below for longitudinal field (Sec. II, diffusion equation) and for perpendicular field (Sec. III, integrodifferential equation). These general equations, however, describe the dynamics of flux motion not only in the *linear* case but also if the resistivity is *nonlinear*, e.g., if ρ depends on the current density. Nonlinear $\rho(J, B, T)$ typically is considered at low frequencies, where the nonlinearity generates higher harmonics with an amplitude depending on the amplitude of the applied ac field. Therefore, an explicit frequency dependence of $\rho(J, B, T)$ is usually not taken into account in the nonlinear response.

What are the effects of a finite thickness d of the film? Obviously, finite d will smear the singularities in the ideal two-dimensional (2D) solutions $J(y)$ and $B(y)$ over a width $\approx d$. Such singularities were obtained, e.g., in Refs. 2-4 for the static Bean model in perpendicular geometry, namely, infinite slopes of $J(y)$ and $B(y)$ at the penetrating flux front, and infinities of $B(y) \sim (|y| - a)^{-1/2}$ at the edges or $\sim \ln||y| - b|$ at the flux front. More such infinities will be obtained below for the linear response at short times (Sec. IV) or large frequencies (Sec. V).

In the nonlinear case, if d exceeds the London penetration depth λ, a current-caused longitudinal Bean critical state[35] may occur across the film thickness as described in Sec. II. The extension of Bean's model to finite λ, which yields a nonlocal relationship between $B_y(x)$ and the flux-line density $n(x)$,[24] is given in Ref. 36. For the static nonlinear case our general treatment of the response of the strip or disk presented in Sec. III reproduces the correct Bean critical state in perpendicular field of Refs. 3,4 even when the current density is not uniform across the specimen thickness, e.g., if there is a constant current-driven usual (longitudinal) Bean state across the thickness of the strip or disk.

In the linear case, when d exceeds the longitudinal ac penetration depth $|\lambda_{\text{ac}}|$ given by $\lambda_{\text{ac}} = (\rho_{\text{ac}}/i\omega\mu_0)^{1/2}$ (Refs. 24,25) with ρ_{ac} from (1.10) or (1.15), the skin ef-

fect increases the sheet resistivity ρ/d above the value ρ_{ac}/d, cf. Sec. II. However, in contrast to the static (or quasistatic) nonlinear case, for which the assumption $d \ll a$ is sufficient, Eq. (1.9) and the expressions of Sec. III do not describe the time-dependent linear response when the film thickness d exceeds $|\lambda_{ac}|$ or (for Ohmic response with real $\rho_{ac} = \rho$) the skin depth $\delta = (2\rho/\omega\mu_0)^{1/2}$. In this case, occurring at large frequencies $\omega \gg 2\rho/\mu_0 d^2$ equivalent to $\delta \ll d$, the ac field and current do *not* penetrate to the center plane $x = 0$ of the film since the specimen behaves as in the Meissner state. In particular, the perpendicular field component B_x vanishes everywhere inside the specimen except very close to the edges (for $a - |y| \gg \delta$). Therefore, our general time- and frequency-dependent theory applies only if $\delta > d$ or $\omega < 2\rho/\mu_0 d^2$, in which case $j(x, y, t)$ and $B(x, y, t)$ are constant over the film thickness. Approximate analytic expressions for the high-frequency case $\delta \ll d$ will be given in Sec. V.

The outline of this work is as follows. In Sec. II some general results for longitudinal geometry are derived and compiled which will be required below. The general equation of motion for the sheet current in thin strips in a time-dependent perpendicular magnetic field is derived in Sec. III, where also an elegant numerical solution method is outlined which accounts for the singularities of the integral kernel and of the solution $J(y)$. The penetration of a sudden change of the applied perpendicular field into an Ohmic strip is considered in Sec. IV, and the linear response of the strip to a perpendicular ac field is calculated in Sec. V. The ac losses are discussed in Sec. VI, and the main results summarized in Sec. VII.

II. DYNAMICS OF LONGITUDINAL CURRENT AND FLUX

A. Diffusion equation

In this section some general results for longitudinal geometry are derived to allow comparison with the results for perpendicular geometry presented in the following sections. I consider the same strip specimen as above ($|x| \leq d/2 \ll a$, $|y| \leq a$, $|z| \leq L/2 \gg a$), but now with field $\mathbf{H}$ and induction $\mathbf{B}$ along $\hat{y}$, and current density $\mathbf{j}$ and electric field $\mathbf{E}$ along $\hat{z}$. H, B, j, and E then depend only on x and t (time). Material parameters enter via Ohm's law

$$E(x, t) = \rho(x, j, B, T) j(x, t) \tag{2.1}$$

and via the reversible magnetization curve $B(H)$ or its slope $\mu(x, B, T) = dB/dH$, which appears in the current equation $\mathbf{j} = (dH/dB)\nabla \times \mathbf{B}$ that in our geometry reads

$$B'(x, t) = \mu(x, B, T) j(x, t) \tag{2.2}$$

($B' = \partial B/\partial x$). Here for generality the superconducting material is allowed to be inhomogeneous, i.e., ρ and μ may depend on x explicitly, in addition to their implicit dependence on x via $j(x)$ (if nonlinear resistivity is considered) and via $B(x)$. With Faraday's law $\dot{\mathbf{B}} = -\nabla \times \mathbf{E}$,

here in the form $\dot{B} = E'$ with $\dot{B} = \partial B/\partial t$, we get from (2.1) and (2.2) the general *nonlinear diffusion equation* for the flux density B,

$$\dot{B}(x, t) = [D(x, t) B'(x, t)]' , \tag{2.3}$$

with diffusivity $D = \rho(x, J, B, T)/\mu(x, B, T)$. The current density obeys a different diffusion equation,

$$\frac{\partial}{\partial t}[\mu(x, t) j(x, t)] = \frac{\partial^2}{\partial x^2}[\rho(x, t) j(x, t)] . \tag{2.4}$$

Note that μ, ρ, and $D = \rho/\mu$ depend implicitly on time t via B and j.

If the applied field $B_a = \mu_0 H_a$ is homogeneous and no current is fed into the strip by contacts, then $B(x) = B(-x)$ is symmetric and $j(x) = -j(-x)$ is antisymmetric. Here I assumed a homogeneous or a symmetrically inhomogenous $[\rho(-x) = \rho(x), \mu(-x) = \mu(x)]$ specimen and used the fact that ρ and μ depend only on the absolute values $|B|$ and $|J|$. In this case one may integrate (2.4), obtaining

$$\rho(x, t) j(x, t) = x\dot{B}_a(t) + \frac{\partial}{\partial t} \int_0^x dx_1$$
$$\times \int_0^{x_1} \mu(x_2, t) j(x_2, t) dx_2 . \tag{2.5}$$

This integrodifferential equation for $j(x, t)$ should be compared with Eq. (3.3) derived below for the sheet current $J(y, t)$ in perpendicular applied field.

B. Nonlinear and linear response

Equations (2.1)–(2.5) may be used to compute j, B, and E (voltage drop) for given nonlinear resistivity ρ and slope μ. In the special case

$$\rho = 0 \text{ for } |j| < j_c(B), \quad \rho = \infty \text{ for } |j| \geq j_c(B) , \tag{2.6}$$

one obtains the critical states of the slab which reduce to the simple Bean model[35] if $j_c(B) = $ const and $\mu(B) = \mu_0$ are assumed. If a smooth nonlinearity is considered, say, $\rho \propto \exp(j/j_1)$ or $\rho \propto \exp(-j_2/j)$, the solution of (2.1)–(2.5) describes flux creep, which may also be called *nonlinear* diffusion.

An equally important example, which will be discussed here in some detail, is the *linear* diffusion of flux, realized in the regimes of the usual flux flow or thermally assisted flux flow or in normal conductors. In this Ohmic case the resistivity is constant and real.

C. Linear response to a field change

Let us first consider the situation where the applied field H_a is suddenly increased by δH_a. This field enhancement and the shielding current then penetrate into the slab diffusively according to $\dot{B} = DB''$ and $\frac{\partial}{\partial t}j = Dj''$. The diffusivity $D = \rho/\mu_0$ is constant in a normal conductor or, in superconductors, if $B \gg B_{c1}$ (such that

the slope $\mu = \mu_0 = $ const; $B_{c1} = \mu_0 H_{c1}$ is the lower critical field) and if $\delta H_a \ll H_a$ (such that the flux flow or TAFF resistivity is constant). In order to simplify the notation here I put $\delta H_a = 1$ and omit the constant background field. Then the jump of H_a at time $t = 0$ is the step function

$$H_a(t) = \theta(t) \; , \qquad (2.7)$$

i.e., $H_a(t < 0) = 0$ and $H_a(t \geq 0) = 1$. The penetrating field $H(x,t)$ may be obtained by expanding the perturbation at $t = 0$ (the rectangular profile $H - H_a = -1$ for $|x| < d/2$, $H - H_a = 0$ for $|x| > d/2$) into a Fourier series with terms $\sim \cos k_n x$ where $k_n = (2n+1)\pi/d$, $n = 0, 1, 2, \ldots$. Due to the diffusion, the amplitudes of these Fourier components decay exponentially with relaxation rates $1/\tau_n = k^2 D$ or explicitly,

$$\tau_n = \tau_0/(2n+1)^2, \quad \tau_0 = d^2/(\pi^2 D) \; . \qquad (2.8)$$

This gives for H and $j = dH/dx$ (Fig. 1),

$$H(x,t) = 1 - \frac{4}{\pi} \sum_{n=0}^{\infty} (-1)^n \frac{\cos[(2n+1)\frac{\pi x}{d}]}{2n+1} e^{-t/\tau_n}, \qquad (2.9)$$

$$j(x,t) = \frac{4}{d} \sum_{n=0}^{\infty} (-1)^n \sin[(2n+1)\pi x/d] e^{-t/\tau_n}. \qquad (2.10)$$

At $t \gg \tau_0$ one has near the edges $j(x,t) \approx \mathrm{sgn}(x)(\pi D t)^{-1/2} \exp(-\xi^2/4Dt)$ with $\xi = d/2 - |x|$. For constant position x away from the edges, the current density $|j(x,t)|$ is zero for both $t = 0$ and $t = \infty$ and has a maximum $j_{\max} \approx 1.32/\xi$ at time $t_{\max} = \xi^2/2D$. This means, at $t \ll \tau_0$, where $H(x,t)$ has not yet penetrated to the center $x = 0$, one has $\int_0^{d/2} j(x,t)\, dx = 1$ ($= H_a$ in real units). But after $t = \tau_0$ this integral decreases with time as $\exp(-t/\tau_0)$.

The magnetic moment $\mathbf{m} = -\hat{\mathbf{y}} M V$ ($V = 2adL = $ slab volume) for $t \geq 0$ becomes (Fig. 2),

$$M(t) = \frac{2}{d} \int_0^{d/2} x j(x,t)\, dx = \frac{2}{\mu_0 d} \int_0^{d/2} B(x,t)\, dx$$

$$= \frac{8}{\pi^2} \sum_{n=0}^{\infty} (2n+1)^{-2} e^{-t/\tau_n} \; . \qquad (2.11)$$

From (2.11) one has $M(t = 0) = 1$ (ideal shielding), and for $t \ll \tau_0$ one gets $M(t) \approx 1 - 4\pi^{-3/2}(t/\tau_0)^{1/2}$. This square-root cusp of $M(t)$ at $t = 0$ is typical for diffusive behavior of B and j. At long times $t \gg \tau_0$ only the slowest (fundamental) mode $n = 0$ survives, yielding $B/\mu_0 \to 1 - (4/\pi)\cos(\pi x/d)\exp(-t/\tau_0)$, $j \to (4/d)\sin(\pi x/d)\exp(-t/\tau_0)$, $M \to (8/\pi^2)\exp(-t/\tau_0)$.
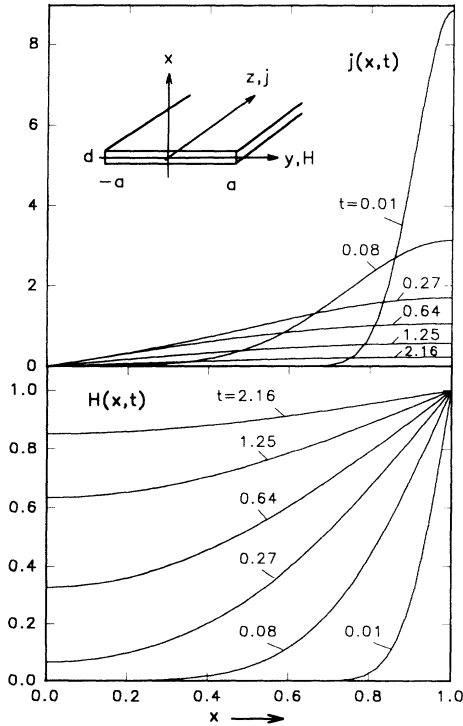

FIG. 1. Diffusive penetration of the current density $j(x,t)$ (2.10) and magnetic field $H(x,t)$ (2.9) into a flat conductor with Ohmic resistivity ρ and thickness d after a longitudinal field $H_a = 1$ is switched on at $t = 0$ (see the inset for the geometry and notation). Shown are the current and field profiles (length unit $d/2 = 1$) at times $t = 0.01$, 0.08, 0.27, 0.64, 1.25, and 2.16 in units $\tau_0 = d^2/\pi^2 D$ (2.8) with $D = \rho/\mu_0$.
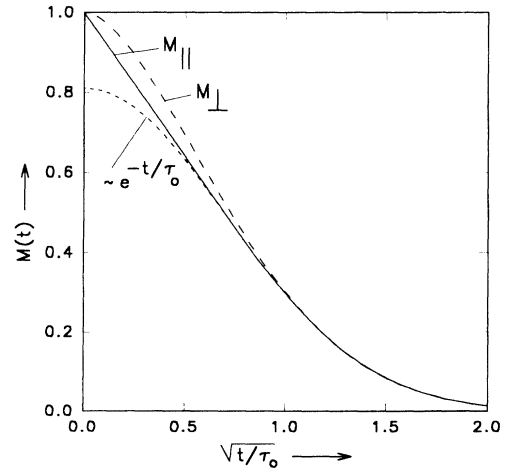

FIG. 2. Magnetic moment $M(t) = M_\parallel(t)$ (2.11) normalized to $M(0) = 1$ for a flat Ohmic conductor after a longitudinal field $H_a = 1$ is switched on at $t = 0$ (solid line). Plotted versus $\sqrt{t}$, $M_\parallel(t)$ becomes a straight line for $t < \tau_0$, and a Gaussian for $t > \tau_0$. For comparison, also shown is the corresponding magnetic moment $M_\perp(t)$ for an Ohmic strip in perpendicular field (long dashes, see Sec. IV below). The time units are $\tau_0 = d^2/\pi^2 D$ (2.8) for $M_\parallel$ and $\tau_0 = 0.249ad/D$ (4.4) for $M_\perp$. Also depicted is the contribution of the slowest eigenmode $(8/\pi^2)\exp(-t/\tau_0)$ (2.11) (short dashes).

D. Linear ac response

Next I consider an applied ac perturbation field,

$$H_a(t) = \exp(i\omega t) . \qquad (2.12)$$

The linear response of the slab is now for the general case of linear complex and dispersive resistivity $\rho_{ac} = i\omega\mu_0\lambda_{ac}^2$ (1.10)[25] (Figs. 3 and 4)

$$H(x,\omega) = \cosh(x/\lambda_{ac})/\cosh(d/2\lambda_{ac}) , \qquad (2.13)$$

$$j(x,\omega) = \lambda_{ac}^{-1}\sinh(x/\lambda_{ac})/\cosh(d/2\lambda_{ac}) , \qquad (2.14)$$

$$M(\omega) = 1 - \frac{2\lambda_{ab}\sinh(x/\lambda_{ac})}{d\cosh(d/2\lambda_{ac})} = 1 - \frac{\tanh u}{u} , \qquad (2.15)$$

where $\lambda_{ac} = (1-i)(\rho_{ac}/2\mu_0\omega)^{1/2}$ is the complex penetration depth and $u = d/2\lambda_{ac}$. From $M(\omega)$ (the negative average magnetic moment per unit volume) one may define

a complex ac susceptibility $\mu(\omega) = \mu' - i\mu''$ normalized to $\mu(\omega = 0) = 1$ and with $\mu(\omega \to \infty) = 0$,

$$\mu(\omega) \equiv 1 - \frac{M(\omega)}{M(\omega \to \infty)} = \frac{\tanh u}{u} . \qquad (2.16)$$

In particular, for Ohmic (real and nondispersive) $\rho_{ac}(\omega) = \rho =$ const, one has $u = d/2\lambda_{ac} = (1 + i)(\omega d^2\mu_0/8\rho)^{1/2} = (1 + i)(\omega\tau_0\pi^2/8)^{1/2}$ and[25,27,37,38]

$$\mu(\omega) = \frac{(\sinh v + \sin v) - i(\sinh v - \sin v)}{v(\cosh v + \cos v)} , \qquad (2.17)$$

with $v = (1 - i)u = (\omega d^2\mu_0/2\rho)^{1/2} = (\omega\tau_0\pi^2/2)^{1/2} = d/\delta$ where $\delta = (2\rho/\mu_0\omega)^{1/2}$ is the skin depth. Writing $\mu = \mu' - i\mu''$ we find that the dissipative part μ'' has a maximum $\mu''_{max} = 0.41723$ at $v = 2.254$, corresponding to $\omega\tau_0 = 1.0295 \approx 1$ and $d/2\delta = 1.127 \approx 1$ or $\omega = \omega_{max} = 10.16\rho/(\mu_0 d^2)$; see Figs. 5 and 6. From (2.16) or (2.17) one has for small and large ω,

$$\mu(\omega) = 1 - \omega^2\tau_0^2\pi^4/120 - i\omega\tau_0\pi^2/12, \quad \omega \ll \tau_0^{-1}, \qquad (2.18)$$

$$\mu(\omega) = (1 - i)(2/\pi^2\omega\tau_0)^{1/2} \sim \omega^{-1/2}, \quad \omega \gg \tau_0^{-1}. \qquad (2.19)$$
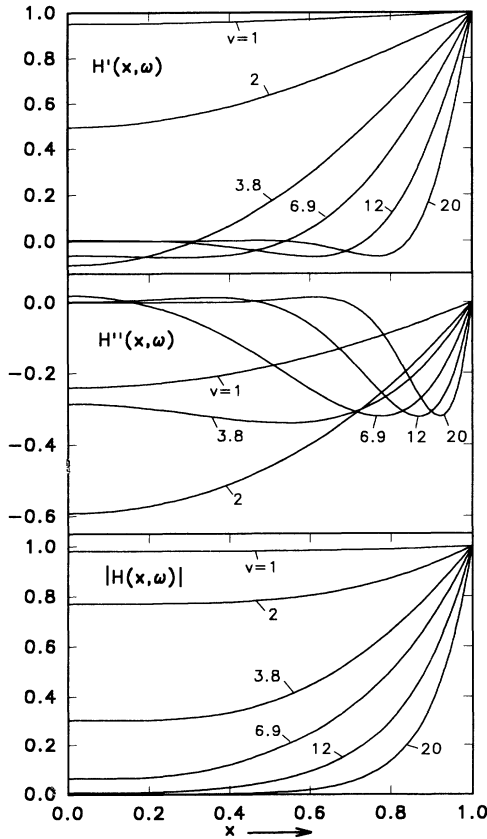

FIG. 3. Complex magnetic field $H(x,\omega) = H' + iH''$ (2.13) inside a superconducting strip of thickness $d = 2$ in longitudinal ac field $H_a(t) = \exp(i\omega t)$. Shown are the real and imaginary parts and the absolute value of H for $v = (\omega d^2/2D)^{1/2} = d/\delta = 1, 2, 3.8, 6.9, 12$, and 20. At $\omega \to 0$ one has full penetration, $H(x,\omega) = H_a$, and at $\omega \to \infty$ the field is completely expelled, $H(x,\omega) = 0$. In this geometry the field outside the strip equals $H_a(t)$, i.e., $H'(x > 1,\omega) = 1$ in our units and $H''(x > 1,\omega) = 0$.
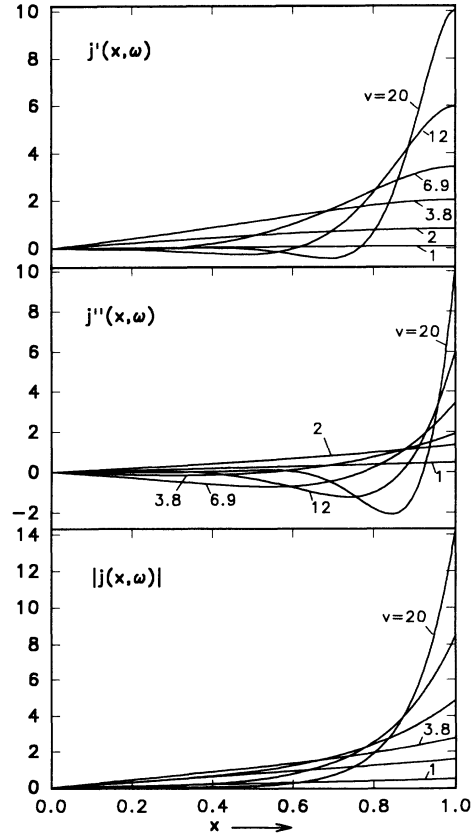

FIG. 4. Complex current density $j(x,\omega) = j' + ij''$ (2.14) in a superconducting strip of thickness $d = 2$ in longitudinal ac field $H_a(t) = \exp(i\omega t)$. Shown are the real and imaginary parts and the absolute value of j for $v = (\omega d^2/2D)^{1/2} = d/\delta = 1, 2, 3.8, 6.9, 12$, and 20. At $\omega \to 0$ the induced current density is zero, and at $\omega \to \infty$ the shielding current is restricted to a thin surface layer.

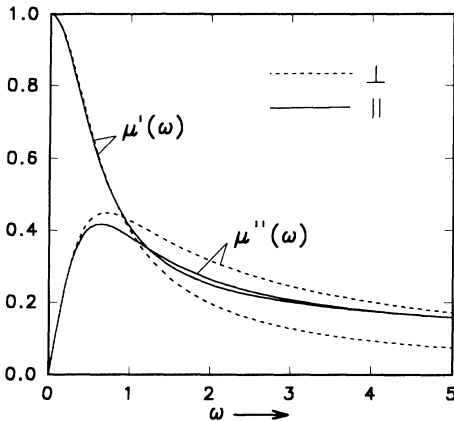FIG. 5. Complex ac susceptibility $\mu(\omega) = \mu_\| = \mu' - i\mu''$ (2.16) of a flat Ohmic conductor in longitudinal ac field (solid lines). For comparison the corresponding $\mu(\omega) = \mu_\perp$ for perpendicular ac field (Sec. V) is also given (dashed lines). The time units are chosen such that the slopes of $\mu_\|''$ and $\mu_\perp''$ at $\omega = 0$ coincide, namely, for $\mu_\perp$ the unit is $\tau = ad/2\pi D$ (3.4) and for $\mu_\|$ the unit is $d^2/16D = \pi^2\tau_0/16$ instead of τ_0 (2.8).

The ac responses (2.13)–(2.16) may be obtained also directly from the responses (2.9)–(2.11) to a steplike perturbation (2.7) by Fourier transformation, noting that the Fourier transform of $\theta(t)$ is $1/i\omega$. In particular, one has the general relationships,

$$M(\omega) = i\omega \int_0^\infty M(t) \exp(-i\omega t)\, dt , \qquad (2.20)$$

$$\mu(\omega) = -M_0^{-1} \int_0^\infty \dot{M}(t) \exp(-i\omega t)\, dt , \qquad (2.21)$$

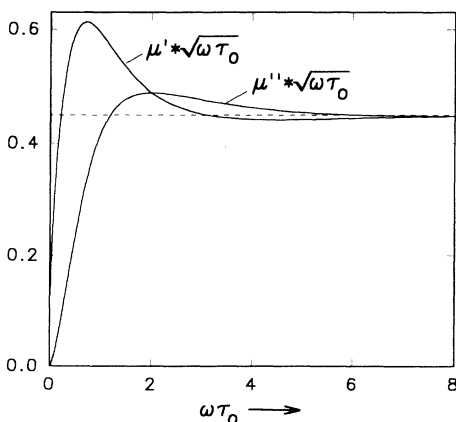where $M_0 = M(t = 0) = M(\omega \to \infty)$. Indeed, from the

FIG. 6. Asymptotic behavior at large frequencies of the complex ac susceptibility $\mu(\omega) = \mu_\| = \mu' - i\mu''$ (2.16) for longitudinal geometry, cf. (2.19). Note that μ' and μ'' at large ω slightly oscillate about the line $(2/\pi^2\omega\tau_0)^{1/2}$ with $\tau_0 = d^2/\pi^2 D$ (2.8).

short-time limit $M(t \ll \tau_0) = 1 - 4\pi^{-3/2}\sqrt{t}$, Eq. (2.21) reproduces the high-frequency limit (2.19). Equations (2.20) and (2.21) will be used in Sec. V to calculate the ac susceptibility of the Ohmic strip in perpendicular field.

E. Frequency-dependent sheet resistivity

If a longitudinal current is applied to the strip then in general the sheet current $J(y)$ (1.1) will not be constant but has to be determined self-consistently as described, e.g., in Refs. 4, 39 for the Bean critical state. A similar inhomogeneous $J(y)$ occurs in the Ohmic case at sufficiently high frequencies. The inhomogeneous $J(y)$ in a strip [or $J(r)$ in a disk and $J(x,y)$ in arbitrarily shaped flat plates] may be applied by contacts or induced by an applied perpendicular field. In all these cases the current-caused magnetic field $\mathbf{H}$ and the current density $\mathbf{j}$ are for linear complex resistivity ρ_{ac} and complex penetration depth $\lambda_{ac} = (\rho_{ac}/i\omega\mu_0)^{1/2}$,

$$\mathbf{H}(x,y,z) = \frac{\mathbf{J}(y,z) \times \hat{\mathbf{x}}}{2} \frac{\sinh(x/\lambda_{ac})}{\sinh(d/2\lambda_{ac})} , \qquad (2.22)$$

$$\mathbf{j}(x,y,z) = \nabla \times \mathbf{H} = \frac{\mathbf{J}(y,z)}{2\lambda_{ac}} \frac{\cosh(x/\lambda_{ac})}{\sinh(d/2\lambda_{ac})} . \qquad (2.23)$$

Note that in the thin specimen considered, $\mathbf{j} = \nabla \times \mathbf{H}$ is not given by the gradient of the perpendicular field, ∇H_x, which is negligible, but by the gradient of the parallel field H_y or H_z, which in the presence of H_x means a curvature of the field lines. The sheet current equals the jump of the parallel field component; if no parallel field is applied one has the surface field $\mathbf{H}(d/2,y,z) = -\mathbf{H}(-d/2,y,z) = \frac{1}{2}\mathbf{J}(y,z) \times \hat{\mathbf{x}}$.

The dissipated power p per unit area caused by the sheet current is obtained by integrating the power density $jE = j^2\rho_{ac}$ over the thickness, or by calculating the Poynting vector $\mathbf{E} \times \mathbf{H}$ at the surface. The result is

$$p(y,z) = J(y,z)^2 \operatorname{Re}\left\{ \frac{\rho_{ac}}{2\lambda_{ac}} \coth\frac{d}{2\lambda_{ac}} \right\} , \qquad (2.24)$$

where $\operatorname{Re}\{z\} = \frac{1}{2}(z + z^*)$ denotes the real part. For Ohmic resistivity p reduces to

$$p(y,z) = J(y,z)^2 \frac{\rho}{4\delta} \frac{\sinh(d/\delta) + \sin(d/\delta)}{\sinh^2(d/2\delta) + \sin^2(d/2\delta)} , \qquad (2.25)$$

with $d/\delta = v = (\omega d^2\mu_0/2\rho)^{1/2}$, cf. (2.17). In the limits of low and high frequencies (2.25) yields

$$p \approx J^2\rho/d \quad \text{for} \quad d/\delta \le 1 , \qquad (2.26)$$

$$p \approx J^2\rho/2\delta \quad \text{for} \quad d/\delta \ge 2 . \qquad (2.27)$$

The dissipation P per unit length of a strip with width $2a$ at large $\omega \gg 2\rho/(\mu_0 d^2)$ (in the ideal screening case $d \ll \delta$) is concentrated near the edges where $J(y)^2 \sim 1/(a - |y|)$ diverges. Introducing a cutoff at $|y| = a - \Delta$, where Δ is of the order of the skin depth δ or thickness

d, we get for a strip with a transport current I the sheet current $J(y) = (I/\pi)(a^2 - y^2)^{-1/2}$ (Refs. 4,39) and the dissipation

$$P = (I^2\rho/2\pi^2 a\delta)\ln(2a/\Delta) . \qquad (2.28)$$

For a strip in a perpendicular ac field H_a one has $J(y) = 2yH_a(a^2 - y^2)^{-1/2}$ (Refs. 3,40) and gets

$$P = (2H_a^2\rho a/2\delta)\,[\ln(2a/\Delta) - 2] . \qquad (2.29)$$

At lower frequencies $2\pi\rho/(\mu_0 ad) \ll \omega < 2\rho/(\mu_0 d^2)$ one still has nearly ideal shielding across the strip width (see below) but, since now $\delta > d$, Eq. (2.26) has to be used; thus in Eqs. (2.28) and (2.29) 2δ is replaced by d. For a strip with transport current this gives

$$P = (I^2\rho/\pi^2 ad)\ln(2a/\Delta) , \qquad (2.30)$$

and for a strip in perpendicular field,

$$P = (2H_a^2\rho a/d)\,\ln(2a/e^2\Delta) , \qquad (2.31)$$

where the cutoff width $\Delta = \Delta(\omega) \approx \rho/(10\mu_0\omega d)$ in (2.30) and (2.31) is obtained in Sec. V.

III. DYNAMICS OF SHEET CURRENT AND OF PERPENDICULAR FLUX

A. Sheet current in a strip

In this section I derive the equation of motion for the sheet current $J(y,t)$ (1.1) flowing in a superconducting or normal-conducting strip to which a time-dependent homogeneous transverse magnetic field $H_a(t)$ is applied (see inset in Fig. 8 below). The small effective penetration field $\sim (d/a)H_{c1}$ and a possible equilibrium magnetization of the material will be disregarded. With these assumptions, a constant applied field penetrates completely as $t \to \infty$. For the perpendicular induction and field components one thus has $B(y,t) = \mu_0 H(y,t)$, where $H(y,t)$ follows from Ampère's law (1.6) for a given sheet current $J(y,t)$. Integrating (1.6) from $y = -y_1$ to $y = y_1$ and noting the symmetry $J(-y) = -J(y)$ of the induced current, one obtains the magnetic flux per unit length threading the strip $|y| \leq y_1$,

$$\phi(y_1) = \frac{\mu_0}{\pi} \int_0^a J(u)\ln\left|\frac{y_1 - u}{y_1 + u}\right| \, du \; + \; 2y_1\mu_0 H_a . \qquad (3.1)$$

When this flux (along $\hat{x}$) changes with time, an electric field $E = \dot{\phi}/2$ (along $-\hat{z}$ like J) is induced at $y = y_1$ and $-E$ at $y = -y_1$. This electric field $E(y,t)$ drives the sheet current $J(y,t) = E(y,t)d(y)/\rho(y)$. With (3.1) inserted one then gets the equation of motion for J (Ref. 40),

$$J(y,t) = \frac{\mu_0 d(y)}{\rho(y)}\left[y\dot{H}_a(t) \right.$$
$$\left. + \frac{1}{2\pi}\int_0^a \dot{J}(u,t)\ln\left|\frac{y-u}{y+u}\right| \, du\right] . \qquad (3.2)$$

With the strip half width a as unit length one may write (3.2) in the form

$$J(y,t) = \tau(y)\frac{\partial}{\partial t}\left[2\pi y H_a(t) \right.$$
$$\left. + \int_0^1 J(u,t)\ln\left|\frac{y-u}{y+u}\right| \, du\right] , \qquad (3.3)$$

with the relaxation time

$$\tau(y) = \mu_0 ad(y)/[2\pi\rho(y)] . \qquad (3.4)$$

In general, $\tau(y)$ may depend on the distance y from the strip axis explicitly via a variable thickness (if the strip cross section is not rectangular) or via an inhomogeneous resistivity $\rho(y)$, or implicitly via the dependence of ρ on $B(y,t)$ and $J(y,t)$. For constant film thickness and linear resistivity, however, τ does not depend on y. Note the similarity of Eqs. (3.3) and (2.5).

Equation (3.3) applies to arbitrary nonlinear resistivity $\rho(J,B)$. In the case of linear, complex resistivity it is more appropriate to express this equation of motion in frequency space in order to account for a possible frequency dependence of $\rho = \rho_{ac}(\omega)$ (which makes the equation nonlocal in the time representation). The Fourier transform $J(y,\omega)$ defined by

$$J(y,t) = \int_{-\infty}^{\infty} J(y,\omega)\exp(i\omega t)\frac{d\omega}{2\pi} , \qquad (3.5)$$

obeys the integral equation

$$J(y,\omega) = i\omega\tau(\omega)\left[2\pi y H_a(\omega) \right.$$
$$\left. + \int_0^1 J(u,\omega)\ln\left|\frac{y-u}{y+u}\right| du\right] , \qquad (3.6)$$

with $\tau(\omega) = \mu_0 ad/[2\pi\rho(\omega)]$.

B. Spatial integration

Both Eq. (3.3) (for nonlinear or linear but nondispersive ρ) and Eq. (3.6) (for linear dispersive ρ) in general have to be solved numerically. Here three problems arise. (a) One is due to the logarithmic singularity of the kernel

$$K(y,u) = \ln\left|\frac{y-u}{y+u}\right| = K(u,y) \qquad (3.7)$$

at $y = u$ and (b) a second to the singularity of the ideal shielding current[3]

$$J_0(y) = 2yH_a/(a^2 - y^2)^{1/2} \qquad (3.8)$$

at $y = \pm a$ (or $y = \pm 1$ if a is the length scale). This ideal shielding current flows either immediately after H_a is switched on $[J(y,t = 0) = J_0(y)]$ or at very large frequencies $[J(y,\omega \gg \tau^{-1}) = J_0(y)]$. A further problem is (c) that the time derivative in (3.3) is on the "wrong" side and thus a direct time integration is not possible. By the same token, a direct iterative solution of (3.6) is

possible only for not too large $\omega\tau$. All these difficulties are overcome by the following numerical solution method, which I describe here for the strip geometry but which works equally well with the disk geometry.

First, substitute in (3.3) for y and u an odd function $y(v) = u(v)$ of a new variable v with $y(0) = 0$, $y(1) = 1$, and $y'(1) = 0$, e.g., $y(v) = u(v) = \frac{3}{2}v - \frac{1}{2}v^3$, which yields the weight function $w(v) = y'(v) = \frac{3}{2}(1 - v^2)$. Then, in order to evaluate the integral as a sum, the new variable v is discretized, e.g., at N equidistant points $v_i = (i - \frac{1}{2})/N$ with $i = 1, 2, ...N$, $N \approx 10...100$. The integral is thus approximated by a sum,

$$\int_0^1 J(u,t)K(y,u)\,du = \int_0^1 J[u(v),t]\,K[y,u(v)]\,w(v)\,dv$$
$$= f[y(v),t]$$
$$\to f_i(t) = \sum_{j=1}^N K_{ij}J_j(t) , \qquad (3.9)$$

with $f_i(t) = f[y(v_i),t]$, $J_j(t) = J[y(v_j),t]$, and

$$K_{ij} = K[y(v_i),u(v_j)]\,w(v_j)/N . \qquad (3.10)$$

This integration method is very accurate. The substitution of the integration variable $u \to u(v)$, $du \to u'(v)dv$, with vanishing weight at the integration boundaries, not only allows one to use equidistant integration points v_i but it also removes the infinity of the integrand $\sim (1-u)^{-1/2}$ occurring for $u \to 1$ at $t = 0$. Note that due to the symmetry of the integrand the point $u = 0$ is not a real integration boundary beyond which the integrand is unknown; therefore, the accuracy of the integration is determined only by the choice of the points $u_i = u(v_i)$ near the boundary $u = 1$.

The definition (3.10) of K_{ij} is not yet complete since with (3.7) for $i = j$ one would get $K_{ii} \sim \ln 0 = \infty$. Thus, K_{ij} (3.10) is valid only for $i \neq j$, and K_{ii} has to be defined separately. One might put $K_{ii} = 0$, but this would cause a large numerical error of order $1/N$. The optimal choice is to determine K_{ii} such that the sum in (3.9) exactly equals the corresponding integral for the special case where J_j =const and the limits of integration extend to infinity. With this choice the integration error decreases with a high power of $1/N$. For $N \gg 1$ one has with Stirling's formula for $N!$,

$$\int_0^{N+\frac{1}{2}} \ln x\,dx - \sum_{i=1}^N \ln i$$
$$\approx \left(N + \frac{1}{2}\right)\left(\ln N + \frac{1}{2N} - 1\right) - \ln(N!)$$
$$\implies -(1/2)\ln(2\pi) \quad \text{for } N \to \infty . \quad (3.11)$$

Using this and accounting for the varying distance of the points $y_i - y_j \approx (i - j)w_i/N$ for $i \approx j$, where $y_i = y(v_i)$ and $w_i = y'(v_i)$, one sees that in the argument of the logarithm the difference $|y_i - y_j|$ for $i = j$ should be replaced by $w_i/2\pi N$. The complete definition of the kernel matrix is thus

$$K_{ij} = \frac{w_j}{N}\ln\left|\frac{y_i - y_j}{y_i + y_j}\right| \quad \text{for } i \neq 0 ,$$
$$K_{ij} = \frac{w_j}{N}\ln\frac{w_j}{4\pi Ny_j} \quad \text{for } i = j . \quad (3.12)$$

C. Time integration

Next I show how the time integration of (3.3) may be performed. Our task is to find the N-vector $J_i(t)$ for all times $t \geq 0$ starting with the known initial function, e.g., $J(y, t = 0) = J_0(y)$ (3.8) if H_a is switched on at $t = 0$, cf. Secs. II and IV. This is achieved by first inverting the matrix K_{ij} (3.12). The inverted matrix K_{ij}^{-1} has to be calculated only once. The general solution J_i of (3.9) for arbitrary f_i then reads

$$J_i(t) = \sum_{j=1}^N K_{ij}^{-1}f_j(t) . \qquad (3.13)$$

Equation (3.3) may now be solved for the time derivative $\dot{J}(y,t)$ by writing it in the form

$$J(y,t)/\tau(y) - 2\pi y\dot{H}_a(t) = \dot{f}(y,t) . \qquad (3.14)$$

Discretizing and inverting this as described above we get

$$\dot{J}_i(t) = \sum_{j=1}^N K_{ij}^{-1}[J_j(t)/\tau_j - 2\pi y_i\dot{H}_a(t)] , \qquad (3.15)$$

where $\tau_j = \tau[y(v_j)]$. Note that τ_j in general depends implicitly on t via B and J. Equation (3.15) for the sheet current $J(y, t)$ is easily integrated by a Runge-Kutta method; for an example, see Sec. IV.

The outlined solution method consists in inverting the integral kernel numerically. For strip geometry, the kernel $K(y, u)$ (3.7) can be inverted also analytically. As shown in Ref. (41), the inversion of Eq. (1.6) is

$$J(y) = \frac{2}{\pi}\int_{-a}^a \frac{H(u) - H_a}{y - u}\left(\frac{a^2 - u^2}{a^2 - y^2}\right)^{1/2}du . \quad (3.16)$$

From this one finds in the Appendix that the equation of motion (3.3) can be written in the equivalent form (with $a = 1$)

$$\frac{\partial J(y,t)}{\partial t} = \frac{2y}{(1-y^2)^{1/2}}\frac{\partial H_a(t)}{\partial t}$$
$$+ \frac{1}{\pi^2}\int_0^1 \frac{2y}{u^2 - y^2}\left(\frac{1 - u^2}{1 - y^2}\right)^{1/2}$$
$$\times \frac{\partial}{\partial u}\frac{J(u,t)}{\tau(u)}\,du . \qquad (3.17)$$

By partial integration Eq. (3.17) may be put into the form $\dot{J}(y,t) = F\{J(y,t)\}$, which may be solved on a grid yielding an equation of motion for the vector $J(y_i, t)$ similar to Eq. (3.15).

D. Magnetic field in a strip

The perpendicular local magnetic field $H(y,t)$ in and near the strip is obtained by inserting the solution $J(y,t)$ of (3.3) or (3.17) into (1.6). In principle, $H(y,t)$ may also be obtained directly as the solution of an integrodifferential equation. The induction law for the strip reads $\mu_0 \dot{H}(y,t) = E'(y,t) = [J(y,t)\rho(y)/d(y)]'$. Inserting here $J(y,t)$ (3.16) one obtains an equation of motion for $H(y,t)$,

$$\dot{H}(y,t) = \frac{2y/\pi^2}{\tau(y)} \int_0^1 \frac{H(u,t) - H_a(t)}{u^2 - y^2} \left(\frac{1-u^2}{1-y^2}\right)^{1/2} du \, .$$

(3.18)

The numerical integration of the diffusionlike Eqs. (3.17) and (3.18) appears to be less stable and less accurate than the integration of our main equation (3.3) by the method outlined above.

E. The circular disk

For a circular disk the equation of motion for the sheet current $J(r,t)$ looks similar to Eqs. (3.3) or (3.6) for the strip; one just has to replace y by the radial coordinate r, the strip half width a by the disk radius R (which may be chosen as unit length), the term $2\pi y H_a$ by $\pi r H_a$, and the integral kernel $K(y,u)$ (3.7) by a more complicated kernel $Q(r,u)$ obtained by integrating the kernel $P(r,u)$ (1.8). Explicitly, one has

$$J(r,t) = \tau(r)\left[\pi r \dot{H}_a(t) + \int_0^1 \dot{J}(u,t)\, Q(r,u)\, du\right] \, , \quad (3.19)$$

$$Q(r,u) = \frac{1}{r} \int_0^r P(r_1,u)\, r_1 \, dr_1 \, , \quad (3.20)$$

$$\tau(r) = \mu_0 R d(r)/[2\pi\rho(r)] \, . \quad (3.21)$$

Both kernels $K(y,u)$ and $Q(r,u)$ for the strip and the disk are dimensionless and depend only on the ratio of their arguments y/u or r/u and are thus easily tabulated. The set of Eqs. (3.19) to (3.21) is completed by Eq. (1.7) for the magnetic field $H(r)$.

Since the equations governing the current and flux dynamics in a strip or disk have the same form, the arguments leading to the equation of motion (3.15) for $J_i(t)$ are the same, and the numerical problems for the two geometries are thus nearly identical.

IV. PENETRATION OF A JUMP IN THE PERPENDICULAR FIELD

In this and the next section I consider the linear problem of the penetration of sheet current and of perpendicular flux into a thin strip with Ohmic (=linear and real) resistivity ρ. This situation is realized in normal conductors and in superconductors in the flux-flow or TAFF

states, cf. Sec. I. We assume here constant thickness, thus $\tau(y) = \tau = \mu_0 ad/2\pi\rho$. As in the longitudinal geometry of Sec. II, the perturbation field is denoted by $H_a(t)$ and performs a step (2.7) or oscillates (2.13) with unit amplitude; a possible constant background field is ignored in our notation.

For a suddenly switched-on field $H_a(t) = \theta(t)$, the sheet current $J(y,t)$ in the strip obeys Eq. (3.3) with initial value $J(y,0)$ (3.8), or explicitly,

$$J(y,t) = 2y/(1-y^2)^{1/2}, \qquad \text{for } t = 0 \, , \quad (4.1)$$

$$J(y,t) = \tau \int_0^1 \dot{J}(u,t)\, K(y,u)\, du \quad \text{for } t \geq 0 \, , \quad (4.2)$$

with $K(y,u) = \ln[|y-u|/(y+u)]$. As in the longitudinal geometry, the general solution to (4.2) is a linear superposition of eigenfunctions $f_n(y)\exp(-t/\tau_n)$ decaying with relaxation times τ_n that are related by $\tau_n = \tau/\Lambda_n$ to eigenvalues Λ_n which follow from the eigenvalue equation

$$f_n(y) = -\Lambda_n \int_0^1 f_n(u)\, \ln\left|\frac{y-u}{y+u}\right| du \, . \quad (4.3)$$

At large times, only the slowest (fundamental) mode $n = 0$ survives. By iterating (4.3) and accounting for the normalization condition $\int_0^1 f_n^2(y)\, dy = 1$ one obtains for this mode $\Lambda_0 = 0.638\,567\,521\,0\ldots$. The fundamental relaxation time of an Ohmic strip is thus

$$\tau_0 = \tau/\Lambda_0 = 0.249\,24\, ad\mu_0/\rho \, . \quad (4.4)$$

This relaxation time was estimated in Ref. 38 as $\tau_0 \approx 2ad\mu_0/(\pi^2\rho)$, which is smaller than the exact value (4.4) by a factor 0.81.

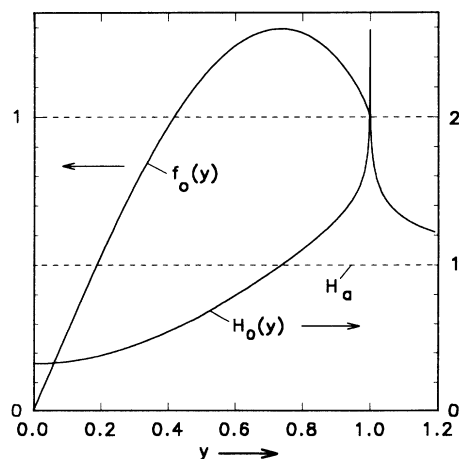The fundamental mode $f_0(y)$ is shown in Fig. 7, to-

FIG. 7. Fundamental eigenfunction $f_0(y)$ of Eq. (4.3) together with the magnetic field $H_0(y)$ obtained by inserting the sheet current $J(y) = f_0(y)$ and the applied field $H_a = 1$ into equation (1.6). At times $t \gg \tau_0$ (4.4) after a constant field H_a is applied, the profiles of the sheet current $J(y,t)$ and field difference $H(y,t) - H_a$ look as depicted here, and their amplitudes decrease as $\exp(-t/\tau_0)$. The amplitudes of $f_0(y)$ and of $H_0(y) - H_a$ have no physical meaning since $f_0(y)$ is normalized.

gether with the corresponding field profile $H_0(y)$. The slope f_0' is $f_0'(0) = 2.7241$ at the strip center and diverges logarithmically at the strip edges as may be seen directly from Eq. (4.3). One has $f(y) \approx 2.724y - 1.724y^3$. Interestingly, it appears that $f_0(1) = 1$ is an exact result, though I did not find a proof for this claim confirmed numerically to eight digits. The rapid convergence of the numerical values for Λ_0 and $f_0(1)$ with increasing N confirms the precision of our solution method and the correct choice of the diagonal elements K_{ii} in the matrix (3.12). At $y = 0.735$, $f_0(y)$ has a maximum $f_{0\,\mathrm{max}} = 1.2965$. Below we shall require $\int_0^1 yf_0(y)\, dy = c_f = 0.5588$.

The higher eigenvalues and eigenfunctions of (4.3) for $n \leq n_{\mathrm{max}} \ll N$ are obtained by diagonalizing the matrix K_{ij} (3.12). Interestingly, one finds $\Lambda_n \approx \Lambda_0 + n$ for all n, and the eigenfunctions look similar to $\sin[(n + \frac{1}{2})\pi x]$. These findings can be proven analytically for $n \gg 1$ by taking the derivative on both sides of (4.3).[42]

Equations (4.1, 4.2) for the sheet current $J(y,t)$ induced by a sudden field change were integrated as described in Sec. III. The resulting $J(y,t)$ and $H(y,t)$ are shown in Fig. 8. At finite times $t > 0$ the $(1 - y^2)^{-1/2}$ infinities of $J(y,t)$ and $H(y,t)$ at the strip edges decrease. The infinity of $J(y,t)$ gets rounded such that the peak moves away from the edge with constant veloc-

ity $v = 0.77\rho/(\mu_0 d)$, which depends only on the specimen thickness d. The field penetration is much faster but such that a weak logarithmic infinity at the edges remains at all times in $H(y,t)$. Of course, all these infinities are smeared when the finite thickness d is accounted for.

The slope $J'(y,t)$ at the strip center initially *increases* as the sheet current penetrates, but after $t = 0.43\tau$ this slope decreases due to the relaxation of the shielding current. At long times $t > 3\tau$ one finds $J(y,t) \approx c_J f_0(y)\exp(-t/\tau_0)$ with $c_J = 2.24$.

Thus, in contrast to the longitudinal geometry of Sec. II, the flux penetration in perpendicular geometry is not a simple diffusion since (a) a logarithmic singularity of $H(y,t)$ persists at the edges, (b) the magnetic field $H(0,t)$ at the center appears more rapidly than with diffusion, (c) the sheet current at all times flows over the entire strip surface, and (d) has a maximum near the edges which initially penetrates with constant velocity and decreases $\sim 1/\sqrt{t}$.

The negative magnetic moment (1.3) calculated from the sheet current is shown in Fig. 2. At $t = 0$ (or $\omega \to \infty$, see Sec. V) one has ideal diamagnetic screening with $M(t = 0) = M(\omega \to 0) = M_0 = \pi a^2 H_a$ (or $M_0 = \pi$ in our units). At short times $t \ll \tau$ one has a logarithmic cusp,

$$M(t)/M_0 \approx 1 + c_1 t \ln(t/c_2\tau),\qquad(4.5)$$

which originates from the large-n modes even as in the longitudinal case of Sec. II where we had a more pronounced square-root cusp. A numerical fit yields $c_1 = 0.205$ and $c_2 = 25.9$[9] We will see in Sec. V that the exact value is $c_1 = 2/\pi^2 = 0.203$. At large times $t > 3\tau$, one has $M(t)/M_0 = c_M \exp(-t/\tau_0)$ with $c_M = 2c_f c_J/\pi = 0.798$, which is close to the corresponding factor $8/\pi^2 = 0.811$ in (2.11).

V. COMPLEX AC SUSCEPTIBILITY IN PERPENDICULAR GEOMETRY

This section treats the linear reponse of the strip to a perpendicular ac field $H_a(t) = \exp(i\omega t)$. The sheet current $J(y)$ follows in this case from the integral equation (3.6) (note that ω is only a parameter),

$$J(y) = i\omega\tau(\omega)\left[2\pi y + \int_0^1 J(u)\,K(y,u)\,du\right],\qquad(5.1)$$

where $\tau(\omega) = \mu_0 ad/2\pi\rho_{\mathrm{ac}}(\omega)$.

In the ideal Meissner state or if pinning is strong, the resistivity (1.10) is imaginary, $\rho_{\mathrm{ac}} = i\omega\mu_0\lambda^2$ (remember λ is the magnetic penetration depth), and thus $i\omega$ cancels in the prefactor $i\omega\tau(\omega) = ad/[2\pi\lambda^2]$ in (5.1). Thus, Eq. (5.1) becomes independent of the frequency and contains only *real* quantities. This means that in the Meissner state the sheet current is in phase with the applied ac field, in contrast to the Ohmic case discussed below. One has here two limiting cases:

(a) If $ad \gg 2\pi\lambda^2$, the term in brackets in (5.1) has to vanish because of the large prefactor. The solution is
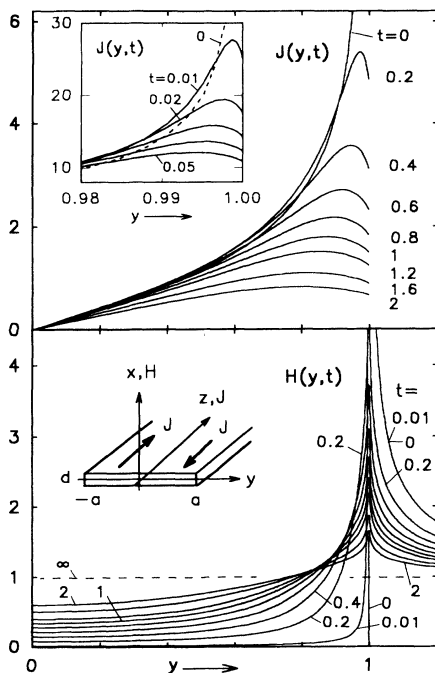

FIG. 8. Penetration of the sheet current $J(y,t)$ and magnetic field $H(y,t)$ into an Ohmic strip of half width $a = 1$ in a perpendicular magnetic field (see lower inset) which is switched on at time $t = 0$. Shown are the profiles at $t = 0$, 0.01, 0.02, 0.03, 0.04, 0.05 (upper inset), and $t = 0.2$, 0.4, 0.6, 0.8, 1, 1.2, 1.6, and 2. At short times and near the edges $J(y,t)$ scales and collapses into one curve if $Jt^{1/2}$ is plotted versus $(1 - y)/t$ as discussed in Sec. VII. Note the logarithmic infinity of $H(y,t)$ at the edge $y = 1$ and the nonconstant $H(y > 1, t)$ outside the strip.

then the ideal screening current (3.8),

$$J(y,t) = 2yH_a(t)/(a^2 - y^2)^{1/2}. \qquad (5.2)$$

(b) If $ad \ll 2\pi\lambda^2$, the screening is incomplete. In this case the solution of (5.1) is

$$J(y,t) = yH_a(t)ad(y)/\lambda^2. \qquad (5.3)$$

Both Eqs. (5.2) and (5.3) apply also to nonperiodic applied field $H_a(t)$ and to spatially varying thickness of the slab. In the nonideal screening case (5.3) it is clearly seen that a strip with *ellipsoidal* cross section $d(y) = d(0)(1 - y^2/a^2)^{1/2}$ *yields a different response* than a strip with constant thickness. While Eq. (5.2) yields the *sheet current* (in this case the strip is much wider than the effective screening length $\lambda_{\text{eff}} = \lambda^2/d \ll 2\pi a$), Eq. (5.3) yields the *current density* $j(y) = J/d = ayH_a/\lambda^2$ (in this case $d \ll 2\pi\lambda^2/a \ll \lambda$).

A similar limit to (5.3) is realized for arbitrary complex or real resistivity at low frequencies $\omega \ll |\tau(\omega)|^{-1}$. One then has $J(y) = i\omega\tau(\omega)2\pi y$, or explicitly for $\rho_{\text{ac}} = \rho$,

$$J(y,t) = (\mu_0 d/\rho)\, y\, \dot{H}_a(t). \qquad (5.4)$$

Equation (5.4) states the well-known fact that the eddy current in a strip is proportional to the distance from the strip center and to the sweep rate of H_a if the sweep is so slow that the field caused by the induced current is negligible. In the opposite limit $\omega \gg |\tau(\omega)|^{-1}$ one has always ideal screening (5.2).

The sheet current for real or complex $\rho_{\text{ac}}(\omega)$ at a given frequency may be obtained by iterating Eq. (5.1) starting with $J(y) = 0$; this procedure corresponds to an expansion of $J(y)$ in powers of the parameter ω and in the Ohmic case converges rapidly for $\omega\tau < 10$. At larger frequencies, faster convergence is achieved by iterating the *inverted* equation, cf. Eqs. (3.15) or (3.17), starting with $J(y) = 2y/(1 - y^2)^{1/2}$, cf. (3.8); this pro-
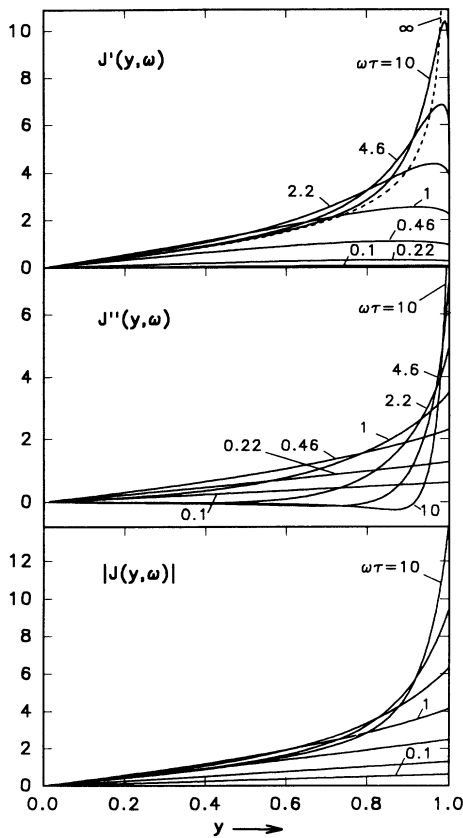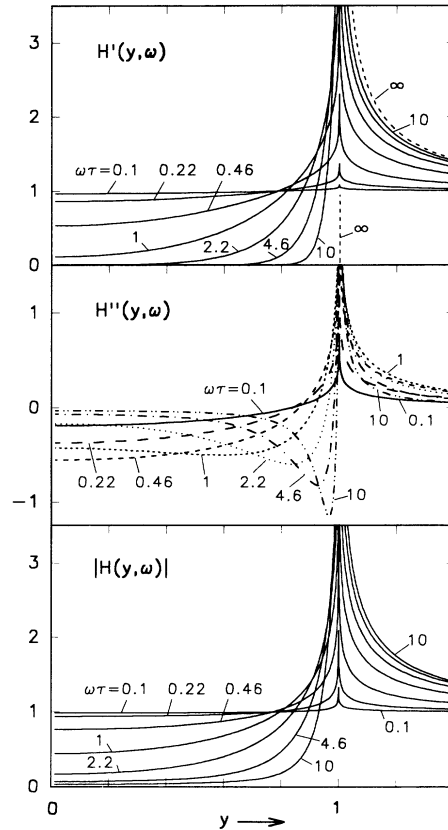

FIG. 10. Complex magnetic ac field $H(y,\omega) = H' + iH''$ obtained from Eqs. (5.1) and (1.6) for an Ohmic strip of half width $a = 1$ in perpendicular ac field $H_a(t) = \exp(i\omega t)$. Shown are the real and imaginary parts and the absolute value of H for $\omega\tau = 0.1$, 0.22, 0.46, 1, 2.2, 4.6, 10, and ∞ with $\tau = ad/2\pi D$ (3.4). Note the logarithmic singularity of $H(y,\omega)$ at the edge $y = 1$. In contrast to longitudinal geometry, the field outside the strip is not constant and has an imaginary part with a nonmonotonic frequency dependence. At $\omega \to 0$ one has full penetration and at $\omega \to \infty$ the field is completely expelled from the strip. At intermediate frequencies $\omega\tau \approx 1$ the out-of-phase part $H''(y,\omega)$ has maximum amplitude both inside and outside the specimen; this observation is related to the maximum in $\mu''(\omega)$.

FIG. 9. Complex ac sheet current $J(y,\omega) = J' + iJ''$ obtained from Eq. (5.1) in an Ohmic strip of half width $a = 1$ in perpendicular ac field $H_a(t) = \exp(i\omega t)$. Shown are the real and imaginary parts and the absolute value of J for $\omega\tau = 0.1$, 0.22, 0.46, 1, 2.2, 4.6, 10, and ∞ with $\tau = ad/2\pi D$ (3.4). As in longitudinal geometry, at $\omega \to 0$ one has full penetration of the field and the induced current is zero. At $\omega \to \infty$ the field is completely expelled and the ideal shielding current of the strip (dashed line) is $J_0(y)$, Eqs. (3.8) and (5.2).

cedure corresponds to an expansion in powers of $1/\omega$ and converges well for $\omega\tau > 3$. Both methods yield exactly the same $J(y)$. To achieve convergence in the iteration of both equations, which have the original form $J(y) = F\{J(y)\}$, these have to be iterated in the form $J(y) \Leftarrow cF\{J(y)\} + (1 - c)J(y)$ with $c < 1$. A small convergence factor $c \ll 1$ is required when the number N of integration points is large and when the expansion parameter $\omega\tau$ or $1/(\omega\tau)$ is large.

The complex ac sheet current $J(y,\omega) = J' + iJ''$ and the corresponding perpendicular field $H(y,\omega) = H' + iH''$ obtained by this iteration are depicted in Figs. 9 and 10. Here J' and H' are the in-phase components, and J'' and H'' are out of phase by $\pi/2$ with respect to the applied field $H_a(t) = \exp(i\omega t)$. $J'(y,\omega)$ looks similar to $J(y,t)$ in Fig. 8, while $H'(y,\omega)$ penetrates more slowly than $H(y,t)$ in Fig. 8. The imaginary parts $J''(y,\omega)$ and $H''(y,\omega)$ depend nonmonotonically on ω as does the dissipative part μ'' of the ac susceptibility shown in Figs. 5 and 11. From (5.1) one gets the expansion

$$J(y) = i\omega\tau 2\pi y + \omega^2\tau^2 2\pi[y + (1-y^2)\mathrm{arctanh}y] + O(\omega^3).$$

(5.5)

The complex magnetic moment $M(\omega) = M' + iM''$ (1.3) may be obtained by integrating $yJ(y,\omega)$ over y for many ω values. In the case of nondispersive ρ or τ, a more convenient way is to use Eqs. (2.20) and (2.21) and integrate the real magnetization $M(t)$ of Sec. IV over ω; the resulting susceptibility $\mu(\omega) = \mu' - i\mu'' = 1 - M(\omega)/M_0$ is shown in Figs. 5 and 11 (remember $M_0 = \pi a^2 H_a$ or $M_0 = \pi$ in our units); μ'' has a maximum $\mu''_{\max} = 0.4488$ at $\omega_{\max} = 0.7074/\tau = 1.108/\tau_0 = 4.445\rho/(\mu_0 ad)$.

The limiting expressions for small and large frequencies are obtained as follows. Inserting (5.5) into (1.3) one gets

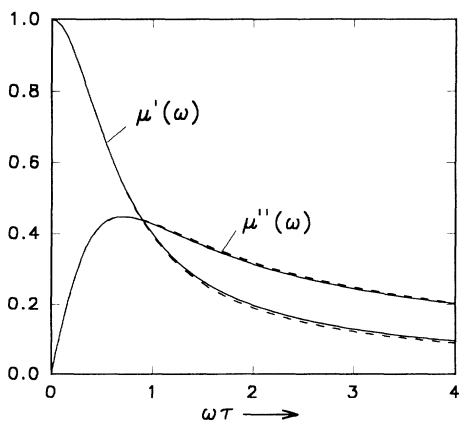$$M(\omega)/M_0 = \tfrac{4}{3}i\omega\tau + 2\omega^2\tau^2 + O(\omega^3);$$

(5.6)

FIG. 11. Complex ac susceptibility $\mu(\omega) = \mu_\perp = \mu' - i\mu''$ of an Ohmic strip in perpendicular ac field, cf. Sec. V (solid lines). The dashed lines give the approximate analytic expressions (5.8) and (5.9), which exhibit the exact asymptotic behavior for large and small frequencies and deviate from the exact result by less than 0.8% or 0.5%.
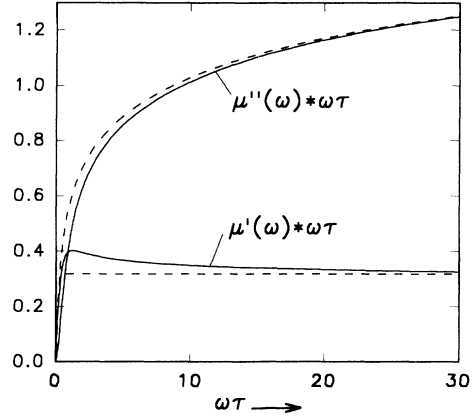

FIG. 12. Asymptotic behavior of the complex ac suscepti-bility $\mu(\omega) = \mu_\perp = \mu' - i\mu''$ (solid lines) for perpendicular geometry at large frequencies. The dashed lines give the lim-iting expression (5.7).

thus $\mu'(\omega) \approx 1 - 2\omega^2\tau^2$ and $\mu''(\omega) \approx \tfrac{4}{3}\omega\tau$. In (5.6) I used the integral $\int_{-1}^{1} du \int_{-1}^{1} dy\,uy\, \ln|y - u| = -1$. The slope of $\mu''(\omega)$ at $\omega = 0$ may be obtained also from (2.21) as $M_0^{-1}\int_0^\infty M(t)\,dt = 4\tau/3$.

A similar direct analytic expansion of $J(y)$ and $M(\omega)$ in powers of $1/\omega$ using Eq. (3.17) fails since all but the zeroth terms (J_0 and M_0) are infinite. However, $M(\omega)$ and $\mu(\omega)$ at large ω may be obtained from the short-time behavior of $M(t)$ (4.5) using Eq. (2.21); this gives

$$\mu(\omega) = c_1\left[\frac{\pi}{2} - i\ln(16.2\omega\tau)\right]/(\omega\tau) + O(\omega^{-2}).$$

(5.7)

The constant 16.2 in the argument of the logarithm is a fit to the numerical result $\mu''(\omega)$ as shown in Fig. 12. The constant c_1 in (4.5) and (5.7) follows from comparison of the dissipation $P = \mu_0 H_a^2\omega\pi a^2\mu''(\omega)$ (Sec. VI) with Eq. (2.31). This yields for the prefactor $c_1 = 2/\pi^2$ and for the cutoff width $\Delta \approx a/(60\omega\tau) = \pi\rho/(30\mu_0\omega d)$.

From the behavior at small and large ω one can con-struct useful analytic expressions which fit $\mu'(\omega)$ and $\mu''(\omega)$ of the strip in a perpendicular ac field in the entire range $-\infty < \omega < \infty$ (cf. the dashed lines in Fig. 11), and which have the correct asymptotic behavior, namely,

$$\mu'(\omega) \approx [1 - c + (c^2 + \pi^2\omega^2\tau^2)^{1/2}]^{-1}, \quad c = \pi^2/4, \quad (5.8)$$

$$\mu''(\omega) \approx \left[\frac{3}{4x} + \frac{\pi^2 x}{\ln(x^2 + 1) + 5.57}\right]^{-1}, \quad x = \omega\tau. \quad (5.9)$$

These surprisingly simple expressions deviate from the exact μ' by less than 8×10^{-3} and from μ'' by less than 5×10^{-3} only. Note that these excellent fits do not contain any fitting parameter apart from the constant $5.57 = 2\ln 16.2$ which was adjusted at $\omega \to \infty$. Similar fits for μ' and μ'' of the disk are given in a forthcoming paper.

VI. ac LOSSES IN A STRIP

In this section I summarize and compare the results for the dissipation P per unit length of a strip in longitudinal

or perpendicular ac magnetic field $H_a \propto \exp(i\omega t)$. Most conveniently, P is calculated from the Poynting vector $\mathbf{E} \times \mathbf{H}$ at the two flat surfaces $x = \pm d/2$,

$$P(t) = -4 \int_0^a E_z \left(\frac{d}{2}, y, z, t\right) H_y \left(\frac{d}{2}, y, z, t\right) dy. \quad (6.1)$$

In ac experiments one is interested in the time-averaged dissipation $P(\omega) = \langle P(t) \rangle$. In complex form, with $E \propto H \propto \exp(i\omega t)$ one has $\langle E(t)H(t) \rangle = \mathrm{Re}\{EH^*\}$. In this section for brevity I denote the time average $\langle H_a^2(t) \rangle$ by H_a^2.

Let us first discuss the linear Ohmic response from above. For *longitudinal* ac field one has (for clarity I use the indices $\parallel$ and $\perp$ in this section)

$$P_{\parallel}(\omega) = 2ad\mu_0 H_a^2 \omega \mu_{\parallel}''(\omega) \quad (6.2)$$

with $\mu_{\parallel}''(\omega)$ from $\mu_{\parallel} = \mu_{\parallel}' - i\mu_{\parallel}''$ (2.17). In particular, $\mu_{\parallel}'' = \omega \tau_{0\parallel} \pi^2/12$ for $\omega \tau_{0\parallel} \ll 1$ and $\mu_{\parallel}'' = (2/\pi^2 \omega \tau_{0\parallel})^{-1/2}$ for $\omega \tau_{0\parallel} \gg 1$ with $\tau_{0\parallel} = \mu_0 d^2/(\pi^2 \rho)$. For *perpendicular* ac field (Sec. V) one has

$$P_{\perp}(\omega) = \pi a^2 \mu_0 H_a^2 \omega \mu_{\perp}''(\omega) \quad (6.3)$$

with $\mu_{\perp}''(\omega)$ (5.9) from the susceptibility $\mu_{\perp} = \mu_{\perp}' - i\mu_{\perp}''$ obtained in Sec. V; one has $\mu_{\perp}'' = 4\omega \tau_{\perp}/3$ for $\omega \tau_{\perp} \ll 1$ and $\mu_{\perp}'' = (2/\pi^2 \omega \tau_{\perp}) \ln(16\omega \tau_{\perp})$ for $\omega \tau_{\perp} \gg 1$ with $\tau_{\perp} = \mu_0 ad/(2\pi \rho)$. The logarithmic factor in $\mu_{\perp}''$ at large frequencies originates from the concentration of the dissipation $J^2(y)\rho$ near the strip edges, cf. Eq. (2.30). At very large frequencies, where the skin depth δ is shorter than $d/2$, the ac losses are given by Eq. (2.29).

Maximum linear ac losses $P_{\max}$ occur at $\omega = \omega_{\max}$,

$$P_{\parallel \,\mathrm{max}} = 2ad\mu_0 H_a^2 \omega_{\max} \times 0.417, \quad (6.4)$$

$$\omega_{\parallel \,\mathrm{max}} = 1.0295\tau_{0\parallel}^{-1} = 10.16\, D/d^2, \quad (6.5)$$

$$P_{\perp \mathrm{max}} = \pi a^2 \mu_0 H_a^2 \omega_{\max} \times 0.449, \quad (6.6)$$

$$\omega_{\perp \mathrm{max}} = 1.108\tau_{0\perp}^{-1} = 8.89\, D/(2ad), \quad (6.7)$$

with $D = \rho/\mu_0$. The maximum linear ac loss per unit length, $P_{\parallel \,\mathrm{max}} = 8.47\mu_0 H_a^2 Da/d$ and $P_{\perp \mathrm{max}} = 6.27\mu_0 H_a^2 Da/d$, is thus largest for longitudinal fields and thin wide films with large resistivity.

The maximum ac loss per cycle, $(2\pi/\omega)P_{\max}$, in both geometries approximately equals the field energy (of density $\mu_0 H_a^2/2$) times 2π times the area $2ad$ or πa^2, respectively. Thus, the ratio of the losses per cycle in the two strip geometries roughly equals the ratio of the cross section $2ad$ to the circular area πa^2. The enhancement factor $\pi a^2/2ad = \pi a/2d$ for perpendicular geometry is caused by the stray field, which is concentrated in a circular tube of radius a around the strip. This factor occurs also in the theory of vibrating superconducting strips or reeds, where it enhances the line tension of a strip with strongly pinned flux lines, as discussed in Refs. 38,43,44.

The magnetic line tension is $2ad\mu_0 H_{\mathrm{dc}}^2$ or $\pi a^2 \mu_0 H_{\mathrm{dc}}^2$, respectively, where H_{dc} is the longitudinal or perpendicular applied field, which is at a right angle to the effective ac field generated by the tilt vibration of the strip.

Equations (6.4)–(6.7) also determine the height and position of the attenuation peaks in vibrating superconductors in oblique magnetic fields where, at sufficiently small vibrational amplitudes, the dissipation originates from various diffusion modes of the flux lines.[38] This prediction was recently confirmed by experiments.[45,46]

For comparison, I give here also the nonlinear ac losses P_{NL} obtained from the original (longitudinal) Bean model[14,47] and from the Bean model for a strip in perpendicular field.[3–5] For the ac losses in a circular disk, see Refs. 2,48,49. A synopsis of these geometries was recently given by Gilchrist.[50] In all these models the critical current density j_c or critical sheet current $J_c = j_c d$ was assumed to be independent of the local induction B, and the slope dB/dH (Sec. II) was put equal to μ_0; this applies for $B \gg B_{c1}$. If $H_a(t)$ cycles between $+H_0$ and $-H_0$, the nonlinear losses equal the area of the hysteresis loop of the magnetization curve times the frequency $\nu = \omega/2\pi$,

$$P_{\mathrm{NL}} = \nu\mu_0 \oint M(H_a)\, dH_a. \quad (6.8)$$

The hysteresis loss per cycle does not depend on the frequency or shape of $H_a(t)$ but only on its amplitude H_m. If $H_a(t) = H_m \cos(\omega t)$ the above factor H_a^2 [e.g., in Eqs. (6.2)–(6.4) and (6.6)] has the value $\langle H_a^2(t) \rangle = \frac{1}{2}H_m^2$.

For longitudinal ac field the Bean model yields the time-averaged dissipation per unit length of a strip,

$$P_{\mathrm{NL}\parallel} = 4ad\nu\mu_0 H_{c\parallel}^2 f(H_m/H_{c\parallel}), \quad (6.9)$$

where $H_{c\parallel} = j_c d/2$ is the field of full penetration and $f(x \leq 1) = x^3/3$, $f(x \geq 1) = x - 2/3$. For a strip in perpendicular ac field one has[3–5]

$$P_{\mathrm{NL}\perp} = 4\pi a^2 \nu\mu_0 H_{c\perp} H_m\, g(H_m/H_{c\perp}), \quad (6.10)$$

where $H_{c\perp} = j_c d/\pi$ and $g(x) = (2/x) \ln \cosh x - \tanh x$ with $g(x \ll 1) \approx x^3/6$ and $g(x \gg 1) \approx 1$, yielding

$$P_{\mathrm{NL}\perp} \approx (a^2\omega/3)\mu_0 H_m^4/H_{c\perp}^2 \sim H_m^4, \quad \text{for } H_m \ll H_{c\perp}. \quad (6.11)$$

Thus, at small ac amplitudes H_m and low frequencies one has for a strip (and disk) the linear losses $P_{\parallel} \sim ad\omega^2 H_m^2$ and $P_{\perp} \sim a^2\omega^2 H_m^2$, whereas the hysteresis losses at small H_m are $P_{\mathrm{NL}\parallel} \sim ad\omega H_m^3$ and $P_{\mathrm{NL}\perp} \sim a^2\omega H_m^4$.

The susceptibility $\mu'' \sim P/(H_m^2\omega)$ in the *linear* case is independent of the ac amplitude H_m but has a maximum at a frequency (6.5) or (6.7). As opposed to this, the *nonlinear* μ'' of the Bean model is independent of ω but is maximum at an amplitude $H_m = H_{\parallel \mathrm{max}} = 4H_{c\parallel}/3 = 0.67j_c d$ or $H_m = H_{\perp \mathrm{max}} = 2.46H_{c\perp} = 0.78j_c d$ for the strip. The corresponding losses are $P_{\mathrm{NL}\parallel} = \frac{2}{3}ad^3\nu\mu_0 j_c^2$ and $P_{\mathrm{NL}\perp} = 1.436a^2 d^2\nu\mu_0 j_c^2$. Interestingly, if nonlinear susceptibilities μ_{NL}'' are defined by (6.2) and (6.3)

(with $H_a^2 = H_m^2/2$) then their maximum values are nearly equal, $\mu''_{\text{NL}\parallel\text{max}} = 3/4\pi = 0.2387$ and $\mu''_{\text{NL}\perp\text{max}} = 0.236\,466\,32\ldots$. This result was obtained also in Ref. 50. The maximum nonlinear μ'' are smaller than the maximum linear μ'', which are also very close in both geometries, $\mu''_{\parallel\text{max}} = 0.417$ and $\mu''_{\perp\text{max}} = 0.435$. For recent discussions of the transition from linear to nonlinear flux diffusion in HTSC's see Refs. 51–53.

VII. SUMMARY AND DISCUSSION

The sheet current $J(y)$ in a conducting thin strip in perpendicular magnetic field $H_a(t)$ follows from the integrodifferential equation (3.3) if the (in general nonlinear) resistivity $\rho = \rho(J)$ is independent of frequency, and from the integral equation (3.6) if $\rho = \rho_{\text{ac}}(\omega)$ is linear and arbitrarily dispersive and complex. The sheet current $J(r)$ in a *disk* obeys Eq. (3.19), which will be solved in a forthcoming paper (Part II). As examples, Ohmic strips in a longitudinal and perpendicular time-dependent field are discussed in detail. The fundamental relaxation time of an Ohmic strip is $\tau_0 = 0.249ad/D$ (4.4).

After a sudden change of the applied field, the penetration of current and field in longitudinal geometry is diffusive, but in perpendicular geometry it has features which are distinct from diffusion. At short times or large frequencies the current densities $j(x,t)$ (2.10) (Fig. 1) and $j(x,\omega)$ (2.14) (Fig. 4) for longitudinal geometry, and the sheet currents $J(y,t)$ (Fig. 8) and $J(y,\omega)$ (Fig. 9) which solve Eqs. (3.3) or (3.6) for perpendicular geometry, *scale* near the surfaces or near the edges of the strip as follows,

$$j(x,t) \approx f_1(\xi/\sqrt{t})/\sqrt{t} \, , \tag{7.1}$$

$$j(x,\omega) \approx f_2(\xi\sqrt{\omega})\sqrt{\omega} \, , \tag{7.2}$$

$$J(y,t) \approx f_3(\eta/t)/\sqrt{t} \, , \tag{7.3}$$

$$J(y,\omega) \approx f_4(\eta\omega)\sqrt{\omega} \, , \tag{7.4}$$

where $\xi = d/2 - |x|$, $\eta = a - |y|$, and f_1, f_2, f_3, and f_4 are universal functions (which in this notation depend on d, a, or $D = \rho/\mu_0$). Therefore, the corresponding curves in Figs. 1, 4, 8, and 9 for (reduced) $t \ll 1$ or $\omega \gg 1$ *collapse into one curve* near $x = 1$ or $y = 1$. These universal functions have the following features: f_1 is a Gaussian centered at the surface; f_2 is an exponential with complex argument and phase $\pi/4$ at the surface; f_3 has a maximum $f_{3,\text{max}} = 2.787H_a\tau^{1/2}$ at $\eta/t = 0.123a/\tau$ and at the edge is $f_3(0) = 2.51H_a\tau^{1/2}$; the real part of f_4 has a maximum $f_{4,\text{max}} = 3.363H_a\tau^{1/2}$ at $\eta/t = 0.074a/\tau$ and at the edge one has $f_4(0) = 3.15(1 + i)H_a\tau^{1/2} = (\pi i)^{1/2}f_3(0)$. These maxima in the sheet current (and parallel field component H_y) near the edges of a thin film should be observable by magneto-optics or by Hall probes.

The different scaling for longitudinal and perpendic-

ular geometry proves the nondiffusive character of the initial penetration of the sheet current $J(y,t)$ from the edges: its maximum initially penetrates with constant velocity $v = 0.123a/\tau = 0.77D/d$ and its height decreases $\sim t^{-1/2}$. This initial penetration velocity is independent of the width and shape of the flat conductor but is a universal feature of thin edges with constant thickness.

The magnetic moment and the ac susceptibility $\mu(\omega)$ are obtained by calculating the complex ac sheet current from (3.19) or by Fourier-transforming the real magnetic moment which relaxes after a sudden field change. Real and imaginary parts of the ac susceptibility look qualitatively similar in both geometries but have different asymptotic behavior at large ω, namely, $\mu_\parallel \sim (1 - i)/\sqrt{\omega}$ (2.19) and $\mu_\perp \sim [\pi/2 - i\ln(16\omega\tau)]/\omega$ (5.7). This means that with increasing frequency the negative phase $\arctan(\mu''/\mu')$ of $\mu(\omega) = \mu' - i\mu''$ goes to $\pi/4$ for longitudinal ac field, but is greater than $\pi/4$ and increases logarithmically for perpendicular ac field. Analytic expressions which approximate $\mu_\perp$ in the entire frequency range are given by (5.8) and (5.9). The ac losses are discussed for linear (Ohmic) and nonlinear (Bean model) response in both geometries. At large frequencies the Ohmic strip screens the applied ac field almost completely, and the losses are given by (2.29) if the skin depth $\delta \ll d$ is small, and by (2.31) if $\delta > d$. The corresponding losses for strips with ac transport currents are given by Eqs. (2.28) and (2.30). The explicit results for the disk will be given in a forthcoming paper.

The present theory in principle allows one to obtain for a strip or disk, by a one-dimensional numerical integration, the nonlinear relaxation (creep) of the sheet current, and the ac response for general complex resistivity $\rho_{\text{ac}}(\omega)$, like (1.10) or (1.15). An efficient integration method is outlined in Sec. III. There remains the challenging task to solve the linear response equations (4.2) or (5.1) analytically.

ACKNOWLEDGMENTS

APPENDIX

The integral equation (3.3) or its integral kernel (3.7) may be inverted in the following way. In general, if two functions $f(y)$ and $g(y)$ are defined in the interval $-1 \le y \le 1$ and are related by

$$f(y) = \int_{-1}^{1} \frac{g(u)}{y - u} du \tag{A1}$$

(all the integrals have to be taken in the sense of Cauchy's principal value) then one has[41]

$$g(y) = \frac{1}{\pi^2} \int_{-1}^{1} \frac{f(u)}{u - y} \left(\frac{1 - u^2}{1 - y^2}\right)^{1/2} du \, . \tag{A2}$$

This inversion follows by conformal mapping; see also Ref. 54. If further

$$h(y) = \int_{-1}^{1} g(u) \ln|y - u|\, du \, , \qquad \text{(A3)}$$

then obviously $h'(y) = f(y)$ (A3). Therefore, Eq. (A2) is solved by (A2) with $f(y)$ replaced by $h'(y)$. In particular, if $f(-y) = f(y)$ is even then $g(-y) = -g(y)$ and thus

$$h(y) = -h(-y) = \int_{0}^{1} g(u) \ln\left|\frac{y-u}{y+u}\right|\, du \, , \qquad \text{(A4)}$$

which is solved by

$$g(y) = \frac{1}{\pi^2} \int_{0}^{1} \frac{2y}{u^2 - y^2} \left(\frac{1-u^2}{1-y^2}\right)^{1/2} h'(u)\, du \, . \qquad \text{(A5)}$$

Thus, the inverse of the integral kernel $K(y, u)$ (3.7) is

$$K^{-1}(y, u) = \frac{2y/\pi^2}{u^2 - y^2} \left(\frac{1-u^2}{1-y^2}\right)^{1/2} \frac{\partial}{\partial u} \, . \qquad \text{(A6)}$$

With (A4) and (A5), Eq. (3.3) can be solved for $\dot{J}(y, t)$,

$$\dot{J}(y, t) = \frac{1}{\pi^2} \int_{-1}^{1} \frac{1}{u-y} \left(\frac{1-u^2}{1-y^2}\right)^{1/2}$$
$$\times \left[-2\pi \dot{H}_a(t) + \frac{\partial}{\partial y} \frac{J(u,t)}{\tau(u)} \right] du \, . \qquad \text{(A7)}$$

Using the formula from Ref. 41,

$$\int_{-1}^{1} \frac{(1-u^2)^{1/2}}{y - u}\, du = \pi y \, , \qquad \text{(A8)}$$

one can rewrite (A7) in the form

$$\dot{J}(y, t) = \frac{2y}{(1-y^2)^{1/2}} \left[\dot{H}_a(t) \right.$$
$$\left. + \frac{1}{\pi^2} \int_{0}^{1} \frac{(1-u^2)^{1/2}}{u^2 - y^2} \frac{\partial}{\partial u} \frac{J(u,t)}{\tau(u)}\, du \right] \, , \qquad \text{(A9)}$$

which is Eq. (3.17).

[1] L. D. Landau and E. M. Lifshitz, *Theoretical Physics, Vol. VIII: Electrodynamics of Continuous Media* (Pergamon, Oxford, 1963).

[2] P. N. Mikheenko and Yu. E. Kuzovlev, Physica C **204**, 229 (1993).

[3] E. H. Brandt, M. Indenbom, and A. Forkl, Europhys. Lett. **22**, 735 (1993).

[4] E. H. Brandt and M. Indenbom, Phys. Rev. B **48**, 13 893 (1993).

[5] M. Darwin, J. Deak, L. Hou, M. McElfresh, E. Zeldov, J. R. Clem, and M. Indenbom, Phys. Rev. B **48**, 13 192 (1993); E. Zeldov, J. R. Clem, M. McElfresh, and M. Darwin (unpublished).

[6] J. Provost, E. Paumier, and A. Fortini, J. Phys. F **4**, 439 (1974).

[7] M. V. Indenbom, H. Kronmüller, T. W. Li, P. H. Kes, and A. A. Menovsky (unpublished).

[8] L. Burlachkov, Phys. Rev. B **47**, 8056 (1993).

[9] E. H. Brandt, Phys. Rev. Lett. **71**, 2821 (1993).

[10] D. J. Frankel, J. Appl. Phys. **50**, 5402 (1979).

[11] M. Daeumling and D. C. Larbalestier, Phys. Rev. B **40**, 9350 (1989).

[12] L. W. Connor and A. P. Malozemoff, Phys. Rev. B **43**, 402 (1991).

[13] H. Theuss, A. Forkl, and H. Kronmüller, Physica C **190**, 345 (1992).

[14] A. M. Campbell and J. Evetts, Adv. Phys. **21** 199 (1972); S. Senoussi, J. Phys. III (France) **2**, 1041 (1992).

[15] M. V. Indenbom, A. Forkl, H.-U. Habermeier, and H. Kronmüller, J. Alloys Compounds **195**, 499 (1993).

[16] Th. Schuster, M. R. Koblischka, B. Ludescher, N. Moser, and H. Kronmüller, Cryogenics **31**, 269 (1991).

[17] L. A. Dorosinskii, M. V. Indenbom, V. I. Nikitenko, Yu. A. Ossip'yan, A. A. Polyanskii, and V. K. Vlasko-Vlasov, Physica C **203**, 149 (1992).

[18] P. Brüll, D. Kirchgässner, and P. Leiderer, Physica C **195**, 157 (1991).

[19] T. K. Worthington, M. P. A. Fisher, D. A. Huse, J. Toner, A. D. Marwick, T. Zabel, C. A. Feild, and F. Holtzberg, Phys. Rev. B **46**, 11 854 (1992).

[20] G. Blatter and V. B. Geshkenbein, Phys. Rev. B **47**, 2725 (1993); G. Blatter, M. V. Feigel'man, V. B. Geshkenbein, A. I. Larkin, and V. M. Vinokur, Rev. Mod. Phys. (to be published).

[21] E. H. Brandt, Physica B **169**, 91 (1991); Int. J. Mod. Phys. B **5**, 751 (1991).

[22] M. W. Coffey and J. R. Clem, Phys. Rev. Lett. **67**, 386 (1991).

[23] M. W. Coffey and J. R. Clem, Phys. Rev. B **45**, 9872 (1992); **45**, 10 527 (1992); **46**, 11 757 (1992); **48**, 342 (1992).

[24] E. H. Brandt, Phys. Rev. Lett. **67**, 2219 (1991); Physica C **185-189**, 270 (1991).

[25] E. H. Brandt, Physica C **195**, 1 (1992).

[26] D. Dew-Hughes, Cryogenics **28**, 674 (1988).

[27] P. H. Kes, J. Aarts, J. van den Berg, C. J. van der Beek, and J. A. Mydosh, Supercond. Sci. Technol. **1**, 242 (1989).

[28] R. Labusch, Cryst. Lattice Defects **1**, 1 (1969); A. M. Campbell, J. Phys. C **2**, 1492 (1969); **4**, 3186 (1971);

[29] B. I. Ivlev, Yu. N. Ovchinnikov, and R. S. Thompson, Phys. Rev. B **44**, 7023 (1991).

[30] G. Blatter, V. B. Geshkenbein, and V. M. Vinokur, Phys. Rev. Lett. **66**, 3297 (1991).

[31] R. Griessen, J. G. Lensink, and H. G. Schnack, Physica C **185-189**, 337 (1991).

[32] R. Behr, J. Kötzler, A. Spirgatis, and M. Ziese, Physica A **191**, 464 (1992).

[33] A. Spirgatis *et al.*, Cryogenics **33**, 138 (1993).

[34] J. Kötzler (unpublished).

[35] C. P. Bean, Rev. Mod. Phys. **36**, 31 (1964); J. Appl. Phys. **41**, 2482 (1970).

[36] L. M. Fisher, I. F. Voloshin, V, S. Gorbachev, S. E. Savel'ev, and V. A. Yampol'skii (unpublished).

[37] V. B. Geshkenbein, V. M. Vinokur, and R. Fehrenbacher,

Phys. Rev. B **43**, 3748 (1991).

[38] E. H. Brandt, Phys. Rev. Lett. **68**, 3769 (1992).

[39] W. T. Norris, J. Phys. D **3**, 489 (1970); see also G. W. Swan, J. Math. Phys. **9**, 1308 (1968).

[40] E. H. Brandt, Z. Phys. B **80**, 167 (1990).

[41] E. H. Brandt, Phys. Rev. B **46**, 8628 (1992).

[42] Yu. N. Ovchinnikov (private communication).

[43] E. H. Brandt, P. Esquinazi, H. Neckel, and G. Weiss, Phys. Rev. Lett. **56**, 89 (1986); J. Low Temp. Phys. **63**, 187 (1986); E. H. Brandt, J. Phys. (Paris) Colloq. **48**, C8-31 (1987).

[44] P. Esquinazi, J. Low Temp. Phys. **85**, 139 (1991).

[45] A. Gupta, Y. Kopelevich, M. Ziese, P. Esquinazi, P. Fisher, F. I. Schultz, and H. F. Braun, Phys. Rev. B **48**, 6359 (1993).

[46] P. Esquinazi and M. Ziese (unpublished).

[47] E. H. Brandt, in *Vortices in Superfluids*, edited by N. Bontemps (Kluwer, Dordrecht, in press).

[48] J. Zhu, J. Mester, J. Lockhart, and J. Turneaure, Physica C **212**, 216 (1993).

[49] J. R. Clem and A. Sanchez (unpublished).

[50] J. Gilchrist, Physica C **219**, 67 (1994).

[51] C. J. van der Beek, V. B. Geshkenbein, and V. M. Vinokur, Phys. Rev. B **48**, 3393 (1993).

[52] A. Gurevich and H. Küpfer, Phys. Rev. B **48**, 6477 (1993).

[53] S. Takács and F. Gömöry, Supercond. Sci. Technol. **3**, 94 (1990); F. Gömöry and S. Takács, Physica C **217**, 297 (1993).

[54] J. R. Clem, R. P. Huebener, and D. E. Gallus, J. Low Temp. Phys. **12**, 449 (1973).